

Advancing Causal Inference: A Nonparametric Approach to ATE and CATE Estimation with Continuous Treatments

Hugo Gobato Souto¹ and Francisco Louzada Neto²

¹Institute of Mathematics and Computer Sciences at University of São Paulo, Brazil
Av. Trab. São Carlense 400, 13566-590 São Carlos (SP), Brazil
hgsouto@usp.br. <https://orcid.org/0000-0002-7039-0572>

²Institute of Mathematics and Computer Sciences at University of São Paulo, Brazil
Av. Trab. São Carlense, 400, São Carlos, 13566-590, Brazil
louzada@icmc.usp.br. <https://orcid.org/0000-0001-7815-9554>

Abstract

This paper introduces a generalized ps-BART model for the estimation of Average Treatment Effect (ATE) and Conditional Average Treatment Effect (CATE) in continuous treatments, addressing limitations of the Bayesian Causal Forest (BCF) model. The ps-BART model's nonparametric nature allows for flexibility in capturing nonlinear relationships between treatment and outcome variables. Across three distinct sets of Data Generating Processes (DGPs), the ps-BART model consistently outperforms the BCF model, particularly in highly nonlinear settings. The ps-BART model's robustness in uncertainty estimation and accuracy in both pointwise and probabilistic estimation demonstrate its utility for real-world applications. This research fills a crucial gap in causal inference literature, providing a tool better suited for nonlinear treatment-outcome relationships and opening avenues for further exploration in the domain of continuous treatment effect estimation.

Key Words : Conditional Average Treatment Effect, Average Treatment Effect, Bayesian Additive Regression Trees, Bayesian Causal Forest Model, Continuous Treatment Effect.

1 Introduction

Causal inference aims to estimate the causal effect of a treatment on an outcome, adjusting for confounding factors that may influence both the treatment assignment and the outcome (Bembom & van der Laan, 2007; Crown, 2019; Cui et al., 2020; Grimmer,

2014; Kuang et al., 2020; Murnane & Willett, 2010; Ohlsson & Kendler, 2020; Sobel, 2000; Yao et al., 2021). In the context of continuous treatments, the estimation of causal effects becomes more complex than in the binary treatment case due to the need to model the treatment effect as a continuous function rather than a fixed difference (Hirano & Imbens, 2004; Lee, 2018; Rothenhäusler & Yu, 2019; Wu et al., 2022).

Consider the potential outcomes framework, which is fundamental in causal inference. Let $Y(d)$ denote the potential outcome corresponding to treatment level $d \in \mathbb{R}$, where D is a continuous treatment variable, and X represents a vector of covariates. The observed outcome for an individual is given by $Y = Y(D)$. The primary objective is to estimate the causal effect of varying the treatment D while controlling for covariates X .

In the case of binary treatments ($D \in \{0, 1\}$), the Average Treatment Effect (ATE) is defined as the difference between the expected potential outcomes:

$$\text{ATE} = \mathbb{E}[Y(1) - Y(0)]. \quad (1)$$

Similarly, the Conditional Average Treatment Effect (CATE) is defined as:

$$\text{CATE}(\mathbf{X} = \mathbf{x}) = \mathbb{E}[Y(1) - Y(0) \mid \mathbf{X} = \mathbf{x}]. \quad (2)$$

For binary treatments, ATE and CATE are scalar quantities, representing the difference in expected outcomes between two discrete levels of treatment.

However, when the treatment variable D is continuous, the causal effect of interest becomes a function of the treatment level (Kennedy et al., 2016; Moodie & Stephens, 2010). The ATE for continuous treatments is expressed as a function of the treatment dose:

$$\phi(D) = \mathbb{E}[Y(D)], \quad (3)$$

where $\phi(D)$ represents the dose-response function. The continuous ATE is often referred to as the dose-response function, which captures the expected outcome as a function of the continuous treatment level. In this context, the estimation challenge shifts from a scalar difference to modeling a function that may exhibit complex nonlinearities depending on the treatment dose.

The CATE for continuous treatments further generalizes the concept of CATE in binary settings (Kennedy et al., 2016; Moodie & Stephens, 2010). It is defined as:

$$\phi(D \mid \mathbf{X} = \mathbf{x}) = \mathbb{E}[Y(D) \mid \mathbf{X} = \mathbf{x}]. \quad (4)$$

This represents the expected outcome as a function of the treatment level D , conditional on the covariates X . Unlike the binary case, where CATE is a scalar for each covariate value, in the continuous case, CATE is a function of both the treatment level and the covariates (Woody et al., 2020). The complexity arises from the fact that this function must account for the interaction between the treatment dose and the covariates, which may vary across different regions of the covariate space.

The estimation of ATE and CATE for binary and continuous treatments involves fundamental differences in both the interpretation and the modeling approach (Kennedy et al., 2016; Moodie & Stephens, 2010; Woody et al., 2020). In the binary treatment case, the estimation typically involves models that predict the difference in outcomes

between the treated and untreated groups, often using methods like propensity score matching or inverse probability weighting (Chernozhukov et al., 2024; Curth & van der Schaar, 2021; Hahn et al., 2020). In the continuous treatment case, on the other hand, the model must capture the entire dose-response relationship, which may involve nonparametric or semi-parametric methods that do not assume a specific functional form for $\phi(D)$ (Kennedy et al., 2016; Moodie & Stephens, 2010; Woody et al., 2020). The complexity increases with the dimensionality of \mathbf{X} , as the conditional treatment effect function $\phi(D | \mathbf{X} = \mathbf{x})$ must be estimated across the covariate space, which can be computationally intensive and requires careful regularization to avoid overfitting (Hirano & Imbens, 2004; Lee, 2018; Rothenhäusler & Yu, 2019; Wu et al., 2022).

Additionally, the interpretation of ATE and CATE varies for binary and continuous treatments. For binary treatments, ATE and CATE provide clear comparisons between two scenarios (treatment vs. no treatment), making the interpretation straightforward (Kennedy, 2020; Künzel et al., 2019; Nie & Wager, 2017). On the other hand, for continuous treatments, the interpretation involves understanding how the expected outcome changes with varying doses of the treatment. The CATE, in particular, requires analyzing how the treatment effect varies not just with the treatment level but also with the covariates. If two individuals have covariates that are close in the covariate space, the difference in their treatment effect functions $\phi(D | \mathbf{X} = \mathbf{x}_1)$ and $\phi(D | \mathbf{X} = \mathbf{x}_2)$ should be small. Conversely, if the covariates are far apart, the treatment effect functions may differ significantly.

These differences necessitate distinct approaches in both the theoretical framework and the empirical modeling strategies for ATE and CATE in the context of continuous treatments. The challenges inherent in estimating these functions, especially the conditional effect $\phi(D | \mathbf{X} = \mathbf{x})$, underscore the need for robust nonparametric methods that can flexibly model the potentially complex relationships between the treatment, covariates, and outcomes.

Despite the growing interest in causal inference for continuous treatments, significant gaps remain in the estimation of the CATE for these treatments (Woody et al., 2020). While there exists a considerable body of literature focusing on the estimation of the ATE for continuous treatments (Hirano & Imbens, 2004; Kennedy, 2020; Künzel et al., 2019; Lee, 2018; Nie & Wager, 2017; Rothenhäusler & Yu, 2019; Wu et al., 2022), the extension to CATE has been comparatively understudied, especially for probabilistic estimations of the CATE functions (Woody et al., 2020). This gap is particularly pronounced given the practical importance of CATE, which allows for the heterogeneity of treatment effects across different levels of covariates \mathbf{X} .

Another critical gap in the current literature is the lack of models that provide probabilistic estimates of ATE and CATE for continuous treatments (Woody et al., 2020). Probabilistic estimation, which includes the construction of confidence intervals (CIs) around the estimates, is crucial for quantifying the uncertainty associated with the treatment effect. Without these intervals, practitioners cannot assess the reliability of the estimates, making it difficult to draw robust conclusions from the data (Woody et al., 2020).

A notable exception in this landscape is the work of Woody et al. (2020), who proposed a generalization of the nonparametric Bayesian Causal Forest (BCF) model to estimate both ATE and CATE for continuous treatments. The BCF model originally

introduced for binary treatments was adapted by Woody et al. (2020) to handle continuous treatments, marking a significant advancement in the field. Nonetheless, to do so, Woody et al. (2020) needed to make the assumption effect of the treatment exposure on the outcome is linear, transforming the generalization of the BCF model into a semi-nonparametric approach.

While their model represents a significant step forward in terms of incorporating uncertainty into the estimation of ATE and CATE for continuous treatments, it does so at the cost of imposing a parametric structure on the relationship between D and Y . This trade-off limits the model’s applicability in scenarios where the treatment effect is not linear, potentially leading to biased estimates when the true relationship deviates from this assumption (i.e., model misspecification) (Cai & Hong, 2003; Hayashi et al., 2011; X. Liu, 2016; Martin & Syring, 2022).

To address this limitation of the BCF model for continuous treatments, this paper proposes a model that generalizes the propensity score Bayesian Additive Regression Trees (ps-BART) model for the estimation of ATE and CATE for continuous treatments. The ps-BART model was initially proposed as a benchmark in the original paper introducing the BCF model by Hahn et al. (2020). However, unlike the BCF model, which incorporates a linear term to model the effect of D on Y , the ps-BART model in its generalized form does not assume that the relationship between D and Y is linear.

The key advantage of the ps-BART model lies in its nonparametric nature. By not imposing a linearity assumption, the model can capture complex interactions and non-linearities that may be present in the data. This is particularly valuable in settings where the treatment effect is expected to vary in a non-monotonic or interaction-dependent manner across different levels of D and different covariate configurations.

The generalized ps-BART model offers several advantages over the BCF model:

1. **Flexibility:** The model’s nonparametric nature allows it to adapt to a wide variety of functional forms, capturing both simple and complex relationships between D , X , and Y .
2. **Accuracy:** By avoiding the imposition of a linear structure, the model reduces the risk of misspecification and bias, particularly in settings where the true treatment effect is nonlinear or involves intricate interactions between covariates.
3. **Generalizability:** The model can be applied to a broad range of DGPs, making it suitable for diverse empirical applications where the nature of the treatment effect is unknown or suspected to be nonlinear.

In summary, this research addresses the current limitations of the existing models for estimation of continuous treatments effect, namely by proposing a fully nonparametric model that can estimate both ATE and CATE functions without the treatment-outcome-linearity assumption while providing CIs for these function estimations. Thereby, this paper contributes to the development of more robust methods in causal inference for continuous treatments effect estimation.

The remainder of this paper is composed of the following sections: Section 2 presents the proposed model for the estimation of continuous treatments effect, while

Section 3 thoroughly describes the experimental design of this research to put the proposed model to the test against the current benchmark model (i.e., the BCF model). Additionally, the results of this paper’s experiments and their respective analysis can be found in Section 4. Finally, Section 5 concludes this paper by presenting the novel insights drawn from the experiments and implications of the results of these experiments.

2 ps-BART for Continuous Treatments

The Bayesian Additive Regression Trees (BART) model, originally developed by Chipman et al. (2010), is a Bayesian ensemble learning technique that constructs a predictive model by summing the outputs of multiple regression trees. Each tree in the ensemble makes a small contribution to the overall prediction, enabling BART to model intricate and nonlinear patterns in the data.

In BART, the response variable Y is modeled as the sum of the outputs from several regression trees, along with an additive error term. This model can be expressed mathematically as:

$$Y_i = \sum_{j=1}^m h_j(\mathbf{x}_i; T_j, M_j) + \epsilon_i, \quad \epsilon_i \sim \mathcal{N}(0, \sigma^2), \quad (5)$$

where Y_i denotes the response for the i -th observation, $h_j(\cdot)$ is the function representing the j -th tree with structure T_j and terminal node parameters M_j , \mathbf{x}_i are the covariates associated with the i -th observation, m is the number of trees, and ϵ_i is the normally distributed error term with zero mean and variance σ^2 . In the Bayesian framework, it is necessary to define priors for the model parameters, including the tree structures T_j , the terminal node parameters M_j , and the variance σ^2 of the errors.

The prior distribution for the tree structure T_j typically involves specifying the probability of a split at each node. This probability is commonly defined as:

$$p(\text{split at node } t) = \alpha(1 + d_t)^{-\beta}, \quad (6)$$

where d_t denotes the depth of node t , and α and β are hyperparameters that control the depth of the tree, often set to 0.95 and 2, respectively (Chipman et al., 2010). For the terminal node parameters M_j , a normal distribution is usually chosen as the prior:

$$\mu_{j,k} \sim \mathcal{N}(\mu_\mu, \sigma_\mu^2), \quad (7)$$

where $\mu_{j,k}$ is the mean response at the k -th terminal node of the j -th tree, and μ_μ and σ_μ^2 are hyperparameters. These hyperparameters are typically set by solving the equations $m\mu_\mu - k\sqrt{m}\sigma_\mu = y_{\min}$ and $m\mu_\mu + k\sqrt{m}\sigma_\mu = y_{\max}$ for a chosen value of k (Chipman et al., 2010). A common choice is $k = 2$, which ensures a 95% prior probability that $\mathbb{E}(Y | x)$ lies within the interval (y_{\min}, y_{\max}) .

The prior for the error variance σ^2 is typically chosen to follow an inverse gamma distribution:

$$\sigma^2 \sim \text{IG}(v/2, v\lambda/2), \quad (8)$$

where ν and λ are hyperparameters. To specify these hyperparameters, a data-driven approach is often employed. This involves calibrating the prior degrees of freedom ν and the scale parameter λ using a rough estimate $\hat{\sigma}$ of σ . Common strategies for estimating $\hat{\sigma}$ include: (1) using the sample standard deviation of Y (the “naive” approach), or (2) using the residual standard deviation from a least squares linear regression of Y on the covariates X (the “linear model” approach), with the latter often providing better calibration (Chipman et al., 2010). A typical value for ν ranges between 3 and 10, which determines the shape of the distribution, and λ is chosen so that the q -th quantile of the prior distribution of σ corresponds to $\hat{\sigma}$, i.e., $P(\sigma < \hat{\sigma}) = q$. Common choices for q are 0.75, 0.90, or 0.99, effectively centering the distribution below $\hat{\sigma}$. The default values for (ν, q) are (3, 0.90) (Chipman et al., 2010).

Additionally, the number of trees m used in the BART model is another hyperparameter, typically set to 200 (Chipman et al., 2010).

Given the prior specifications and the likelihood function, the posterior distribution of the BART model parameters can be obtained via Markov Chain Monte Carlo (MCMC) methods. The objective is to sample from the joint posterior distribution:

$$p(T_1, M_1, \dots, T_m, M_m, \sigma^2 \mid Y, X). \quad (9)$$

The MCMC procedure for BART generally involves the following steps:

1. **Initialization:** Begin by initializing the tree structures T_j , the terminal node parameters M_j , and the error variance σ^2 .
2. **Gibbs Sampling:** Each tree structure and terminal node parameter is updated iteratively using Gibbs sampling, while conditioning on the other trees and the observed data. Specifically, for each tree j :
 - The tree structure T_j is updated using a Metropolis-Hastings step.
 - The terminal node parameters M_j are updated by sampling from their full conditional posterior distribution.
3. **Update Error Variance:** The error variance σ^2 is updated from its full conditional posterior distribution.
4. **Repeat:** These steps are repeated over many iterations to ensure that the samples converge to the posterior distribution.

Upon convergence of the MCMC algorithm, predictions can be obtained by averaging the posterior samples of the trees.

The ps-BART model, on the other hand, is an extension of the BART framework designed to address specific challenges in causal inference, particularly those arising from Regularization-Induced Confounding (RIC). The ps-BART model enhances the BART model by incorporating an estimated propensity score, which is itself obtained through a BART model, to adjust for potential confounding effects that may distort the estimation of treatment effects (Hahn et al., 2020).

RIC is a phenomenon that occurs in Bayesian models where regularization, imposed through prior distributions or model structures, influences the posterior distribution of treatment effects in unintended ways (Hahn et al., 2018). The core of the RIC

issue lies in the fact that multiple functional forms may yield similar likelihoods but imply vastly different causal effects. This ambiguity becomes particularly problematic in contexts characterized by strong confounding and relatively modest treatment effects (Hahn et al., 2018).

Consider a scenario where the conditional expectation of the outcome variable Y , given the covariates \mathbf{X} and treatment D , is predominantly determined by the covariates rather than the treatment, leading the posterior distribution of the treatment effect to be heavily influenced by the prior over the conditional expectation function (Hahn et al., 2018). This issue is exacerbated in scenarios where treatment assignment is based on predictions of the outcome in the absence of treatment—a situation known as target selection. Here, the covariates \mathbf{X} are used to assign treatment D based on predicted outcomes $\mathbb{E}[Y \mid \mathbf{X} = \mathbf{x}, D = 0]$, creating a feedback loop that strengthens the confounding effect. Consequently, the posterior estimate of the treatment effect can be significantly biased, as the regularization inadvertently confounds the estimated relationship between D and Y (Hahn et al., 2018).

To address the challenges posed by RIC, the ps-BART model incorporates an estimated propensity score $\hat{\pi}(\mathbf{x})$ into the BART framework (Hahn et al., 2020). The propensity score, defined as the conditional probability of receiving treatment given the covariates, $\pi(\mathbf{x}) = P(D = d \mid \mathbf{X} = \mathbf{x})$, is estimated using a separate BART model. Given the fact that we are dealing with a continuous treatment, it is better to use the estimated CDF of the conditional probability of receiving treatment given the covariates, namely $\pi(\mathbf{x}) = P(D \leq d \mid \mathbf{X} = \mathbf{x})$. This score captures the treatment assignment mechanism, allowing the model to account explicitly for confounding factors.

The inclusion of the propensity score $\hat{\pi}(\mathbf{x})$ in the outcome model modifies the BART framework as follows:

$$Y_i = \sum_{j=1}^m h_j(\mathbf{x}_i, d_i, \hat{\pi}(\mathbf{x}_i); T_j, M_j) + \epsilon_i, \quad (10)$$

where $h_j(x_i, \hat{\pi}(\mathbf{x}_i); T_j, M_j)$ represents the j -th regression tree, which now takes both the covariates \mathbf{x}_i , the treatment dose d_i , and the estimated propensity score $\hat{\pi}(\mathbf{x}_i)$ as inputs. The inclusion of $\hat{\pi}(\mathbf{x}_i)$ helps disentangle the effect of the treatment from the effect of the covariates, thereby reducing the influence of RIC.

By incorporating $\hat{\pi}(\mathbf{x}_i)$, the ps-BART model effectively adjusts for the treatment assignment process, mitigating the risk that the prior over the conditional expectation function $f(\mathbf{x}_i)$ overly influences the posterior distribution of the treatment effect. This adjustment is particularly crucial in cases where target selection is present, as it ensures that the model remains robust against the feedback loop created by the treatment assignment mechanism.

After the ps-BART model has been properly trained, the ATE and CATE functions as described in Section 1 can be approximated using the following formulations:

$$\hat{\phi}(D) = \sum_{j=1}^m h_j(\bar{\mathbf{x}}, D, \hat{\pi}(\bar{\mathbf{x}}); T_j, M_j) \quad (11)$$

$$\hat{\phi}(D \mid \mathbf{X} = \mathbf{x}_i) = \sum_{j=1}^m h_j(\mathbf{x}_i, D, \hat{\pi}(\mathbf{x}_i); T_j, M_j) \quad (12)$$

where, $\bar{\mathbf{x}}$ is the empirical mean of the covariates \mathbf{x} . By estimating $\hat{\phi}(D)$ and $\hat{\phi}(D | \mathbf{X} = \mathbf{x}_i)$ for a considerable number of points and interpolating them, we can approximate the real ATE and CATE functions (where the quality of this approximation depends on the performance of the ps-BART model). Additionally, given the bayesian aspect of the ps-BART model, we can also estimate CIs for $\hat{\phi}(D)$ and $\hat{\phi}(D | \mathbf{X} = \mathbf{x}_i)$.

3 Experimental Design

3.1 Data Generating Processes (DGPs) for Model Evaluation

To rigorously evaluate the performance of the proposed ps-BART model in comparison to the benchmark BCF model, a comprehensive experimental design was implemented. This design involved the use of nine distinct DGPs, each carefully constructed to test the models under various conditions that mimic real-world scenarios in causal inference. The DGPs were designed to span a range of complexities, including linear and nonlinear relationships between the treatment and outcome, as well as varying levels of confounding.

The nine DGPs employed in this study were structured to assess the models across different sample sizes and simulation conditions. Specifically, for each DGP, datasets were generated with 100, 250, and 500 observations. Additionally, each scenario was subjected to 100 independent simulations to ensure the robustness and generalizability of the results. This approach resulted in a total of 2,700 distinct datasets, providing a broad basis for comparison between the ps-BART and BCF models.

The first four DGPs are extensions of the model initially proposed by Hirano and Imbens (2004), which was later refined by Moodie and Stephens (2010). Though Moodie and Stephens (2010) also enhanced this DGP by introducing a temporal component, allowing for the consideration of time-dependent effects, this study does not make use of this temporal component for the DGP. Thus, the DGP used for this study is given as:

1. Let X_1 and X_2 be independent random variables drawn from an exponential distribution with rate parameter $\lambda = 1$:

$$X_1 \sim \text{Exp}(1), \quad X_2 \sim \text{Exp}(1).$$

2. Define a constant α , where $\alpha \in \{1, 2, 4, 8\}$.
3. The treatment variable D is generated as a random variable from an exponential distribution with a rate parameter that depends on X_1 and X_2 :

$$D \sim \text{Exp}\left(\frac{\alpha}{X_1 + X_2}\right).$$

4. The outcome variable Y is generated from a normal distribution where the mean is a function of D , X_1 , and X_2 , and the standard deviation is 1:

$$Y \sim \mathcal{N}(D + (X_1 + X_2) \exp(-D \cdot (X_1 + X_2)), 1).$$

By changing the α value, one can increase the nonlinearity and heterogeneity aspect of the continuous treatment effect of the DGP by increasing α . Thus, the choice of various α values, which differs from the proposed DGP of Moodie and Stephens (2010), allows us to test the ps-BART and BCF models for different levels of nonlinearity and heterogeneity of the continuous treatment effect. Given the fact that (semi-)parametric models outperform nonparametric models when correctly specified for the underlying DGP (Jabot, 2015; W. Liu & Yang, 2011; Robinson, 2010), it is already expected that the relative performance of the ps-BART model will improve as the α values increase. Thus, the choice of multiple α values is to determine to the extent of treatment-outcome relationship nonlinearity where the ps-BART model becomes superior over the BCF model.

Moving to the next three DGPs employed in this research, they are based on those proposed by Wu et al. (2022). These DGPs are specifically designed to capture more complex, nonlinear relationships between the treatment and the outcome, incorporating interaction terms and higher-order polynomial effects. They are structured as:

1. Let C_1, C_2, C_3, C_4 be independent random variables drawn from a standard normal distribution, and let C_5 and C_6 be independent random variables drawn from uniform distributions with specified ranges:

$$C_1, C_2, C_3, C_4 \sim \mathcal{N}(0, 1), \quad C_5 \sim \text{Unif}(-2, 2), \quad C_6 \sim \text{Unif}(-3, 3).$$

2. The treatment variable D is generated based on the following model specifications, depending on the scenario $\text{spec} \in \{1, 2, 3\}$:

- Specification 1:

$$D = 9(0.8 + 0.1C_1 + 0.1C_2 - 0.1C_3 + 0.2C_4 + 0.1C_5) - 3 + \epsilon_D,$$

where $\epsilon_D \sim \mathcal{N}(0, 5)$.

- Specification 2:

$$D = 15(0.8 + 0.1C_1 + 0.1C_2 - 0.1C_3 + 0.2C_4 + 0.1C_5) + 2 + 2\epsilon_D,$$

where $\epsilon_D \sim t_4$ (Student's t-distribution with 4 degrees of freedom).

- Specification 3:

$$D = 15(0.8 + 0.1C_1 + 0.1C_2 - 0.1C_3 + 0.2C_4 + 0.1C_5) + 3\sqrt{2}C_3^2 + \epsilon_D,$$

where $\epsilon_D \sim t_4$ (Student's t-distribution with 4 degrees of freedom).

3. The outcome variable Y is generated as a function of D and the confounders C_1, C_2, C_3, C_4, C_5 . The true mean function μ_{DC} is defined as:

$$\mu_{DC} = -10 - (2C_1 + 2C_2 + 3C_3 - C_4 + 2C_5) - D(0.1 - 0.1C_1 + 0.1C_4 + 0.1C_5 + 0.1C_3^2) + 0.13D^3.$$

The outcome Y is then drawn from a normal distribution with mean μ_{DC} and standard deviation $\sqrt{10}$:

$$Y \sim \mathcal{N}(\mu_{DC}, \sqrt{10}).$$

The final two DGPs used in the experimental design are derived from the heterogeneous nonlinear DGP presented by Hahn et al. (2020). The first DGP is given as:

1. Let X_1, X_2, X_3 be independent random variables drawn from a standard normal distribution, X_4 be a categorical variable taking values from $\{1, 2, 3\}$ with equal probability, and X_5 be a binary variable taking values from $\{0, 1\}$ with equal probability:

$$X_1, X_2, X_3 \sim \mathcal{N}(0, 1), \quad X_4 \sim \text{Categorical}\{1, 2, 3\}, \quad X_5 \sim \text{Bernoulli}(0.5).$$

2. The treatment variable D is generated as an exponential random variable, where the rate parameter is a function of the absolute values of X_1, X_2 , and X_3 , along with X_5 :

$$D \sim \text{Exp}\left(\frac{\alpha}{|X_1| + X_5 + |X_2 - X_3|}\right),$$

where $\alpha = 2$.

3. The treatment effect $\tau(X_2, X_5)$ is defined as:

$$\tau(X_2, X_5) = 1 + 2X_2X_5.$$

4. The baseline outcome function $\mu(X_4, X_1, X_3)$ is defined as:

$$\mu(X_4, X_1, X_3) = -6 + g(X_4) + 6|X_3 - 1|.$$

where

$$g(X_4) = \begin{cases} 2, & \text{if } X_4 = 1, \\ -1, & \text{if } X_4 = 2, \\ -4, & \text{if } X_4 = 3. \end{cases}$$

5. The outcome is computed as:

$$Y = \mu(X_4, X_1, X_3) + D \cdot \tau(X_2, X_5).$$

Concerning the second DGP, it follows the exact same structure of the first one with the difference that the outcome is computed as:

$$Y = \mu(X_4, X_1, X_3) + \log(D) \cdot \tau(X_2, X_5).$$

Hence, the first DGP inspired by the heterogeneous nonlinear DGP presented by Hahn et al. (2020) has a continuous treatment that has a linear relationship with the outcome variable while the second DGP has a continuous treatment that has a nonlinear relationship with the outcome variable. Given the fact that (semi-)parametric models outperform nonparametric models when correctly specified for the underlying DGP (Jabot, 2015; W. Liu & Yang, 2011; Robinson, 2010), it is already expected that the BCF model outperforms the ps-BART model for the first DGP. Thus, the choice of this DGP is to determine to what extent the BCF model outperforms the ps-BART model when its key parametric assumption is correctly met.

3.2 Evaluation Metrics and Approach

To rigorously assess the performance of the proposed ps-BART model in comparison to the benchmark BCF model, a set of carefully selected evaluation metrics is employed based on the proposed methodological practices of Souto and Neto (2024).

The primary objective in evaluating the models is to compare the estimated treatment effect functions, denoted as $\hat{\phi}(D)$ for ATE and $\hat{\phi}(D, \mathbf{x}_i)$ for CATE, with the true underlying treatment effect functions $\phi(D) = \mathbb{E}[Y \mid \mathbf{X} = \mathbb{E}[\mathbf{X}], D]$ for ATE and $\phi(D, \mathbf{x}_i) = \mathbb{E}[Y \mid \mathbf{X} = \mathbf{x}_i, D]$ for CATE. Needless to say, it would be computationally impossible to consider all possible values of D when comparing the estimated treatment effect functions with the actual functions given the fact that D is continuous. Hence, both the values of D considered for the model evaluation are 250 values ranging from 0 (no treatment) to the empirical maximum value of D in the j -th simulation for each DGP.

To quantify the accuracy of the models' estimates, three standard error metrics are used: Root Mean Squared Error (RMSE), Mean Absolute Error (MAE), and Mean Absolute Percentage Error (MAPE). These metrics provide a comprehensive assessment of the distance between the true treatment effect ϕ and the estimated effect $\hat{\phi}$:

$$\text{RMSE}_j = \sqrt{\frac{1}{n} \sum_{i=1}^n (\hat{\phi}(D_i, \cdot) - \phi(D_i, \cdot))^2},$$

where j represents the j -th simulation of the considered DGP, n is the number of observations and \cdot in $\hat{\phi}(D_i, \cdot)$ and $\phi(D_i, \cdot)$ is replaced by $\mathbb{E}[\mathbf{X}]$ and \mathbf{x}_i when considering ATE and CATE respectively. RMSE gives greater weight to larger errors, making it sensitive to outliers and useful for evaluating the overall accuracy of the model.

$$\text{MAE}_j = \frac{1}{n} \sum_{i=1}^n |\hat{\phi}(D_i, \cdot) - \phi(D_i, \cdot)|,$$

which measures the average magnitude of the errors without considering their direction. MAE is a straightforward measure of prediction accuracy and is less sensitive to outliers than RMSE.

$$\text{MAPE}_j = \frac{100\%}{n} \sum_{i=1}^n \left| \frac{\hat{\phi}(D_i, \cdot) - \phi(D_i, \cdot)}{\phi(D_i, \cdot)} \right|,$$

where MAPE expresses the error as a percentage, providing an intuitive measure of relative prediction accuracy, particularly useful when the scales of $\phi(D_i, \cdot)$ vary, which is the case here given the different DGPs used in this study.

In addition to point estimates, it is essential to evaluate the models' ability to provide reliable probabilistic estimates of ATE and CATE, particularly in terms of confidence intervals. Two key metrics are used for this purpose:

1. Coverage is defined as the proportion of times the true treatment effect $\phi(D)$ falls within the estimated confidence interval $[\hat{\phi}_{\text{lower}}(D), \hat{\phi}_{\text{upper}}(D)]$, which in this study is the confidence interval of level 95%. Mathematically:

$$\text{Cover}_j = \frac{1}{n} \sum_{i=1}^n \mathbb{I}(\phi(D_i) \in [\hat{\phi}_{\text{lower}}(D_i), \hat{\phi}_{\text{upper}}(D_i)]),$$

where $\mathbb{I}(\cdot)$ is the indicator function. Ideal coverage would match the nominal confidence level, in this study 95%.

2. The length of the confidence interval provides information about the precision of the estimate:

$$\text{Len}_j = \frac{1}{n} \sum_{i=1}^n (\hat{\phi}_{\text{upper}}(D_i) - \hat{\phi}_{\text{lower}}(D_i)).$$

Shorter intervals indicate more precise estimates, although this must be balanced against the coverage to avoid overly narrow intervals that exclude the true effect.

Besides this two key (and commonly used) metrics for uncertainty estimation evaluation, we employ the Squared Error for Coverage (SEC) and Absolute Error for Coverage (AEC) as additional metrics given their complementary power for model uncertainty estimation evaluation (Souto & Neto, 2024):

$$\text{SEC}_j = \frac{1}{n} \sum_{i=1}^n (\text{Cover}_j - \alpha)^2$$

$$\text{AEC}_j = \frac{1}{n} \sum_{i=1}^n |\text{Cover}_j - \alpha|$$

Furthermore, as proposed by Souto and Neto (2024) not only the average values of the chosen evaluation metrics is presented for each DGP (as commonly done in the literature), but also their respective standard deviation values. Additionally, statistical tests are performed to estimate whether the differences in average and standard deviation of the selected metrics between the ps-BART model and the benchmark model are statistically significant or not. The choice for these tests follow the algorithm proposed by Souto and Neto (2024), which considers the statistical properties of every metric results for each DGP to choose the proper set of statistical tests. The considered statistical tests for the algorithm are: 1. T-test, 2. Mann-Whitney U test, 3. Brown-Forsythe test, and 4. Fligner-Policello test for the average values of each metric and 1. F-test, 2. Levene's test, and 3. Brown-Forsythe test for standard deviations of every metric.

4 Results and Analysis

The analysis of the results present in this section has the aim to be concise and to-the-point to ensure the sparsity of this paper. Hence, the results of individual metrics will not be discussed in the details but rather their joint results with the division of point-wise estimation performance measures and uncertainty estimation performance measures. It is worth noting that when we say below that a DGP is (non)linear, we mean that the DGP has a (non)linear relationship between the treatment and outcome

4.1 1st Set of DGPs

4.1.1 $\alpha = 1$

Table 1 presents the results of all metrics for the 1st Set of DGPs with $\alpha = 1$. Starting with $n = 100$, considering the point-wise estimation performance metrics, both

models have a similar performance, with the BCF model being more robust in ATE function estimation than the ps-BART model. Moving to the uncertainty estimation performance measures, it can be seen that the ps-BART model is considerably better in ATE function estimation and slightly better in CATE function estimation. Now moving to $n = 250$ and $n = 500$, the ps-BART model becomes clearly superior in both point-wise estimation and uncertainty estimation, while remaining less robust than the BCF model for ATE function point-wise estimation.

Figures 1, 2, 3, 4, 5, and 6 graphically illustrate the results of Table 1. The misspecification of the BCF model for the underlying DGPs can be visually seen in these figures.

The statistical tests results for $n = 100$, $n = 250$, and $n = 500$ can be seen in Tables 2, 3, and 4 respectively. For $n = 100$, we can infer that the BCF model is statistically significantly better and more robust than the ps-BART model for ATE function point-wise estimation, while being having a similar performance for CATE function point-wise estimation. Regarding uncertainty estimation, the ps-BART model is statistically significantly superior to the BCF model. For $n = 250$ and $n = 500$, it can be concluded that the superiority of the proposed model is statistically significant, while remaining less robust than the BCF model for ATE function point-wise estimation.

Table 1: Metric Results

n	Metric	BCF (Mean \pm SD)	ps-BART (Mean \pm SD)
100	RMSE _{ATE}	0.630 \pm 0.156	0.630 \pm 0.266
	MAE _{ATE}	0.473 \pm 0.108	0.477 \pm 0.258
	MAPE _{ATE}	0.241 \pm 0.058	0.242 \pm 0.145
	Len _{ATE}	1.917 \pm 0.338	3.007 \pm 0.584
	Cover _{ATE}	0.869 \pm 0.092	0.984 \pm 0.043
	RMSE _{CATE}	1.374 \pm 0.783	1.391 \pm 0.875
	MAE _{CATE}	1.132 \pm 0.651	1.103 \pm 0.681
	MAPE _{CATE}	0.149 \pm 0.043	0.156 \pm 0.039
	Len _{CATE}	5.392 \pm 2.187	5.243 \pm 2.005
	Cover _{CATE}	0.936 \pm 0.084	0.954 \pm 0.069
	SEC _{ATE}	0.015 \pm 0.033	0.003 \pm 0.006
	AEC _{ATE}	0.095 \pm 0.079	0.048 \pm 0.026
	SEC _{CATE}	0.007 \pm 0.021	0.005 \pm 0.010
	AEC _{CATE}	0.052 \pm 0.045	0.052 \pm 0.045
250	RMSE _{ATE}	0.567 \pm 0.074	0.484 \pm 0.169
	MAE _{ATE}	0.445 \pm 0.047	0.382 \pm 0.172
	MAPE _{ATE}	0.235 \pm 0.026	0.201 \pm 0.101
	Len _{ATE}	1.298 \pm 0.169	2.412 \pm 0.279
	Cover _{ATE}	0.753 \pm 0.102	0.980 \pm 0.066
	RMSE _{CATE}	1.453 \pm 0.713	1.175 \pm 0.637
	MAE _{CATE}	1.188 \pm 0.595	0.901 \pm 0.462
	MAPE _{CATE}	0.119 \pm 0.032	0.108 \pm 0.020
	Len _{CATE}	3.905 \pm 1.153	5.163 \pm 1.603
	Cover _{CATE}	0.825 \pm 0.156	0.980 \pm 0.034
	SEC _{ATE}	0.049 \pm 0.051	0.005 \pm 0.020
	AEC _{ATE}	0.197 \pm 0.102	0.055 \pm 0.048
	SEC _{CATE}	0.040 \pm 0.066	0.002 \pm 0.003
	AEC _{CATE}	0.136 \pm 0.146	0.041 \pm 0.019
500	RMSE _{ATE}	0.572 \pm 0.073	0.397 \pm 0.157
	MAE _{ATE}	0.433 \pm 0.032	0.309 \pm 0.134
	MAPE _{ATE}	0.228 \pm 0.017	0.160 \pm 0.079
	Len _{ATE}	1.026 \pm 0.114	1.810 \pm 0.255
	Cover _{ATE}	0.682 \pm 0.118	0.962 \pm 0.067
	RMSE _{CATE}	1.684 \pm 0.922	1.179 \pm 1.373
	MAE _{CATE}	1.381 \pm 0.781	0.918 \pm 1.096
	MAPE _{CATE}	0.105 \pm 0.021	0.084 \pm 0.023
	Len _{CATE}	3.343 \pm 1.396	5.653 \pm 3.129
	Cover _{CATE}	0.642 \pm 0.148	0.987 \pm 0.025
	SEC _{ATE}	0.086 \pm 0.079	0.005 \pm 0.011
	AEC _{ATE}	0.268 \pm 0.118	0.054 \pm 0.040
	SEC _{CATE}	0.117 \pm 0.088	0.002 \pm 0.003
	AEC _{CATE}	0.308 \pm 0.148	0.042 \pm 0.015

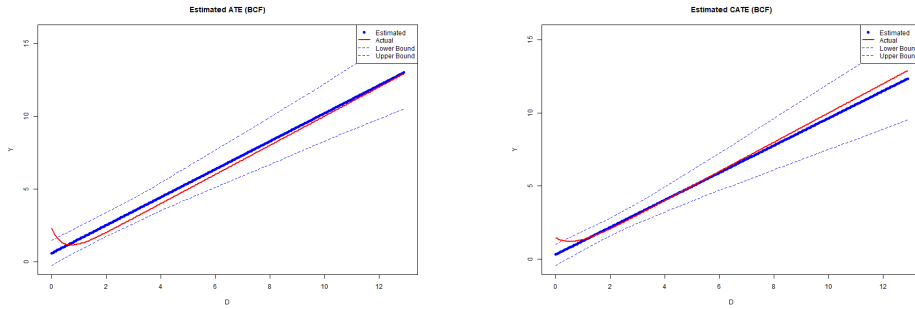


Figure 1: BCF ATE and CATE Functions Estimation for $N=100$ (for CATE, an Example of a Random \mathbf{x}_i of a Random Simulation is used)

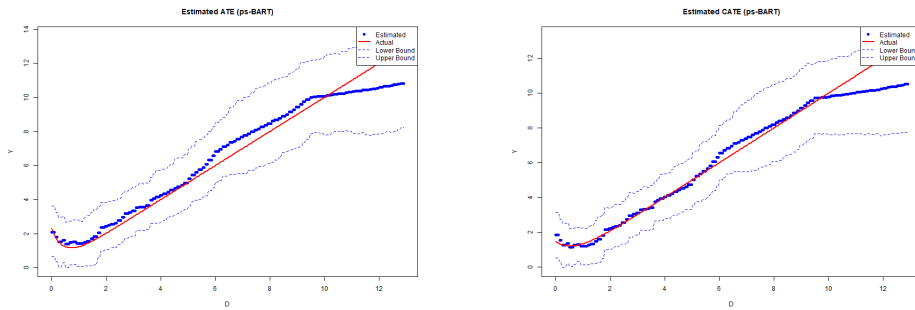


Figure 2: ps-BART ATE and CATE Functions Estimation for $N=100$ (for CATE, an Example of a Random \mathbf{x}_i of a Random Simulation is used)

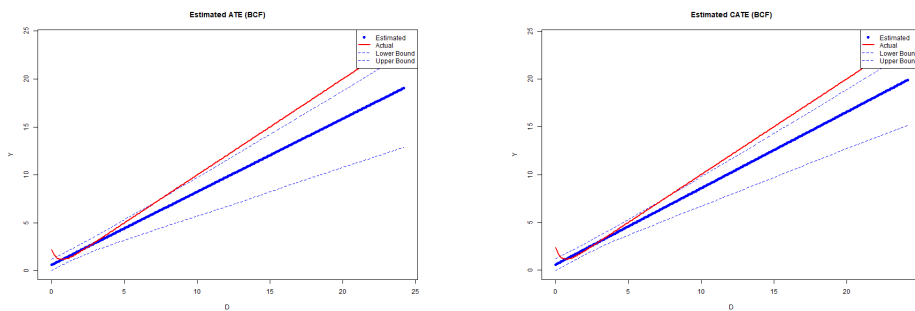


Figure 3: BCF ATE and CATE Functions Estimation for $N=250$ (for CATE, an Example of a Random \mathbf{x}_i of a Random Simulation is used)

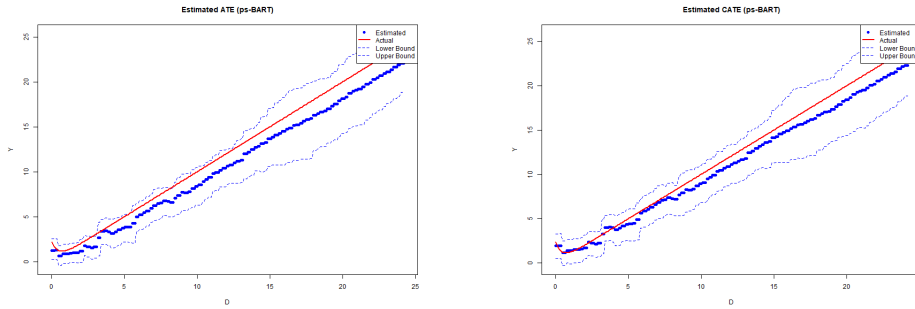


Figure 4: ps-BART ATE and CATE Functions Estimation for $N=250$ (for CATE, an Example of a Random x_i of a Random Simulation is used)

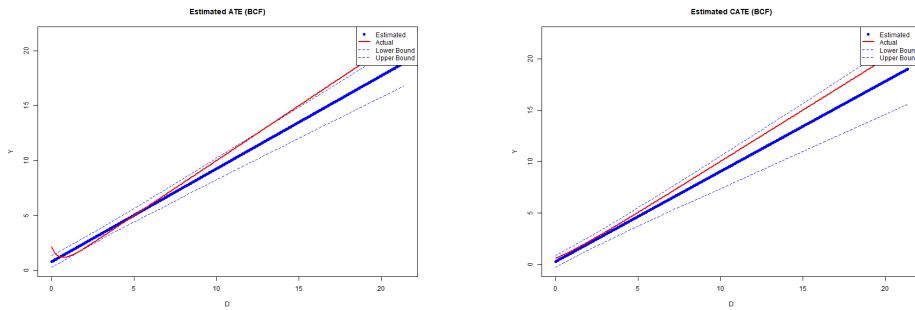


Figure 5: BCF ATE and CATE Functions Estimation for $N=500$ (for CATE, an Example of a Random x_i of a Random Simulation is used)

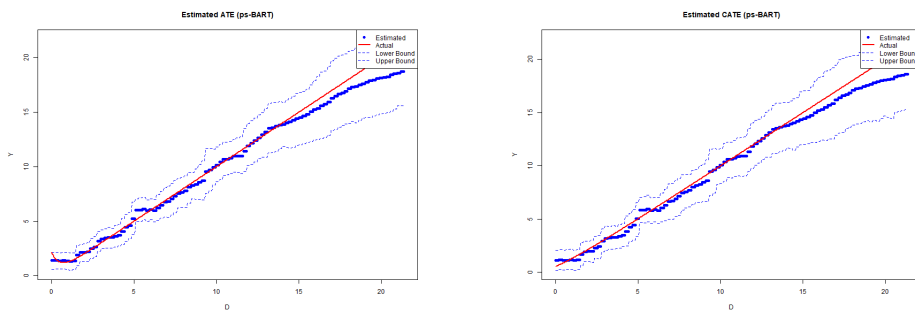


Figure 6: ps-BART ATE and CATE Functions Estimation for $N=500$ (for CATE, an Example of a Random x_i of a Random Simulation is used)

Table 2: Statistical Test Results: p-values for Different Metrics (n=100)

Metric	Fligner-Policello Test	Mann-Whitney U Test	Kruskal-Wallis H Test	Levene's Test	Brown-Forsythe Test
RMSE _{ATE}	0.1338	N/A	N/A	0.000109	0.000596
MAE _{ATE}	0.0220	N/A	N/A	2.65×10^{-7}	1.99×10^{-5}
MAPE _{ATE}	0.0231	N/A	N/A	2.77×10^{-9}	6.74×10^{-7}
Len _{ATE}	N/A	4.57×10^{-30}	4.50×10^{-30}	2.58×10^{-6}	4.14×10^{-6}
RMSE _{CATE}	0.6647	N/A	N/A	0.2794	0.4782
MAE _{CATE}	N/A	0.4082	0.4075	0.5982	0.7866
MAPE _{CATE}	N/A	0.1430	0.1426	0.4742	0.3471
Len _{CATE}	0.7898	N/A	N/A	0.2908	0.4035
SEC _{ATE}	N/A	3.31×10^{-5}	3.29×10^{-5}	1.18×10^{-5}	0.000282
AEC _{ATE}	8.01×10^{-5}	N/A	N/A	5.04×10^{-13}	5.08×10^{-12}
SEC _{CATE}	0.00039	N/A	N/A	0.0112	0.2046
AEC _{CATE}	0.00039	N/A	N/A	0.0434	0.2495

Table 3: Statistical Test Results: p-values for Different Metrics (n=250)

Metric	Fligner-Policello Test	Mann-Whitney U Test	Kruskal-Wallis H Test	Levene's Test	Brown-Forsythe Test
RMSE _{ATE}	2.91×10^{-9}	N/A	N/A	3.91×10^{-10}	1.29×10^{-7}
MAE _{ATE}	2.99×10^{-8}	N/A	N/A	5.50×10^{-14}	2.33×10^{-9}
MAPE _{ATE}	3.16×10^{-8}	N/A	N/A	7.67×10^{-15}	6.15×10^{-11}
Len _{ATE}	0	N/A	N/A	1.72×10^{-5}	1.78×10^{-5}
RMSE _{CATE}	N/A	0.0020	0.0020	0.1332	0.1472
MAE _{CATE}	4.61×10^{-5}	N/A	N/A	0.0128	0.0229
MAPE _{CATE}	0.0201	N/A	N/A	9.81×10^{-5}	0.00021
Len _{CATE}	5.20×10^{-15}	N/A	N/A	0.0136	0.0380
SEC _{ATE}	8.13×10^{-178}	N/A	N/A	1.36×10^{-16}	3.38×10^{-10}
AEC _{ATE}	8.13×10^{-178}	N/A	N/A	1.76×10^{-17}	1.48×10^{-13}
SEC _{CATE}	0.04598	N/A	N/A	8.68×10^{-20}	7.48×10^{-9}
AEC _{CATE}	0.04598	N/A	N/A	4.08×10^{-30}	2.18×10^{-18}

Table 4: Statistical Test Results: p-values for Different Metrics (n=500)

Metric	Fligner-Policello Test	Mann-Whitney U Test	Kruskal-Wallis H Test	Levene's Test	Brown-Forsythe Test
RMSE _{ATE}	3.72×10^{-30}	N/A	N/A	8.56×10^{-8}	2.04×10^{-5}
MAE _{ATE}	1.00×10^{-18}	N/A	N/A	6.27×10^{-20}	1.29×10^{-11}
MAPE _{ATE}	5.35×10^{-15}	N/A	N/A	4.10×10^{-22}	1.56×10^{-12}
Len _{ATE}	0	N/A	N/A	2.95×10^{-5}	3.16×10^{-5}
RMSE _{CATE}	N/A	2.07×10^{-11}	2.05×10^{-11}	0.8922	0.7538
MAE _{CATE}	N/A	3.99×10^{-13}	3.96×10^{-13}	0.6488	0.5230
MAPE _{CATE}	N/A	4.14×10^{-13}	4.11×10^{-13}	0.3527	0.2743
Len _{CATE}	3.99×10^{-40}	N/A	N/A	5.39×10^{-4}	0.00356
SEC _{ATE}	0	N/A	N/A	9.15×10^{-23}	1.08×10^{-11}
AEC _{ATE}	0	N/A	N/A	8.30×10^{-19}	3.17×10^{-12}
SEC _{CATE}	1.05×10^{-57}	N/A	N/A	1.05×10^{-27}	2.43×10^{-25}
AEC _{CATE}	1.05×10^{-57}	N/A	N/A	4.25×10^{-25}	6.36×10^{-24}

4.1.2 $\alpha = 2$

The simulation results for $\alpha = 2$ can be found in 5. For all considered n values, regarding the point-wise estimation performance measures, the ps-BART model is now superior to the BCF model, though the latter remains more robust for ATE function estimation. Moving to the uncertainty estimation performance metrics, it can be seen that the ps-BART model is considerably better in both ATE and CATE function estimation. Such results were already expected as by increasing the α value, we increase the nonlinearity relationship between the treatment and the outcome, increasing the misspecification level of the BCF model and thus favoring the fully-nonparametric ps-BART model.

Figures 7, 8, 9, 10, 11, and 12 graphically illustrate the results of Table 5. The misspecification of the BCF model for the underlying DGPs can be visually seen in these figures.

The statistical tests results for $n = 100$, $n = 250$, and $n = 500$ can be found in Tables 6, 7, and 8 respectively. It can be inferred that the superiority of the ps-BART model is statistically significant, while remaining less robust than the BCF model for ATE function point-wise estimation.

Table 5: Metric Results

n	Metric	BCF (Mean \pm SD)	ps-BART (Mean \pm SD)
100	RMSE _{ATE}	0.572 \pm 0.135	0.471 \pm 0.180
	MAE _{ATE}	0.429 \pm 0.097	0.355 \pm 0.181
	MAPE _{ATE}	0.241 \pm 0.063	0.205 \pm 0.120
	Len _{ATE}	1.356 \pm 0.249	2.155 \pm 0.391
	Cover _{ATE}	0.788 \pm 0.109	0.978 \pm 0.072
	RMSE _{CATE}	1.289 \pm 0.748	1.083 \pm 0.560
	MAE _{CATE}	1.040 \pm 0.616	0.866 \pm 0.444
	MAPE _{CATE}	0.231 \pm 0.069	0.215 \pm 0.055
	Len _{CATE}	3.572 \pm 1.526	3.432 \pm 1.075
	Cover _{CATE}	0.867 \pm 0.137	0.900 \pm 0.116
	SEC _{ATE}	0.038 \pm 0.040	0.006 \pm 0.031
	AEC _{ATE}	0.168 \pm 0.099	0.053 \pm 0.057
	SEC _{CATE}	0.025 \pm 0.050	0.016 \pm 0.029
	AEC _{CATE}	0.099 \pm 0.125	0.087 \pm 0.091
250	RMSE _{ATE}	0.539 \pm 0.087	0.369 \pm 0.146
	MAE _{ATE}	0.413 \pm 0.043	0.289 \pm 0.150
	MAPE _{ATE}	0.235 \pm 0.025	0.174 \pm 0.101
	Len _{ATE}	0.980 \pm 0.131	1.836 \pm 0.226
	Cover _{ATE}	0.640 \pm 0.094	0.986 \pm 0.048
	RMSE _{CATE}	1.669 \pm 0.765	0.960 \pm 0.405
	MAE _{CATE}	1.348 \pm 0.634	0.742 \pm 0.299
	MAPE _{CATE}	0.231 \pm 0.059	0.156 \pm 0.032
	Len _{CATE}	3.082 \pm 0.970	3.370 \pm 0.857
	Cover _{CATE}	0.664 \pm 0.183	0.943 \pm 0.071
	SEC _{ATE}	0.105 \pm 0.061	0.004 \pm 0.011
	AEC _{ATE}	0.310 \pm 0.094	0.051 \pm 0.032
	SEC _{CATE}	0.115 \pm 0.115	0.005 \pm 0.013
	AEC _{CATE}	0.287 \pm 0.182	0.051 \pm 0.049
500	RMSE _{ATE}	0.552 \pm 0.080	0.316 \pm 0.114
	MAE _{ATE}	0.410 \pm 0.031	0.251 \pm 0.109
	MAPE _{ATE}	0.230 \pm 0.019	0.149 \pm 0.071
	Len _{ATE}	0.785 \pm 0.085	1.572 \pm 0.170
	Cover _{ATE}	0.531 \pm 0.097	0.988 \pm 0.036
	RMSE _{CATE}	2.108 \pm 1.080	0.914 \pm 0.715
	MAE _{CATE}	1.714 \pm 0.912	0.712 \pm 0.578
	MAPE _{CATE}	0.227 \pm 0.043	0.123 \pm 0.028
	Len _{CATE}	2.971 \pm 1.162	3.662 \pm 1.678
	Cover _{CATE}	0.476 \pm 0.137	0.970 \pm 0.038
	SEC _{ATE}	0.185 \pm 0.082	0.003 \pm 0.004
	AEC _{ATE}	0.419 \pm 0.097	0.048 \pm 0.021
	SEC _{CATE}	0.243 \pm 0.117	0.002 \pm 0.003
	AEC _{CATE}	0.474 \pm 0.137	0.037 \pm 0.022

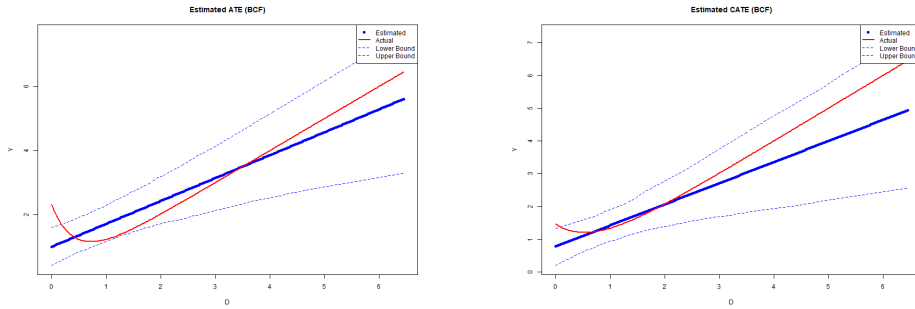


Figure 7: BCF ATE and CATE Functions Estimation for $N=100$ (for CATE, an Example of a Random \mathbf{x}_i of a Random Simulation is used)

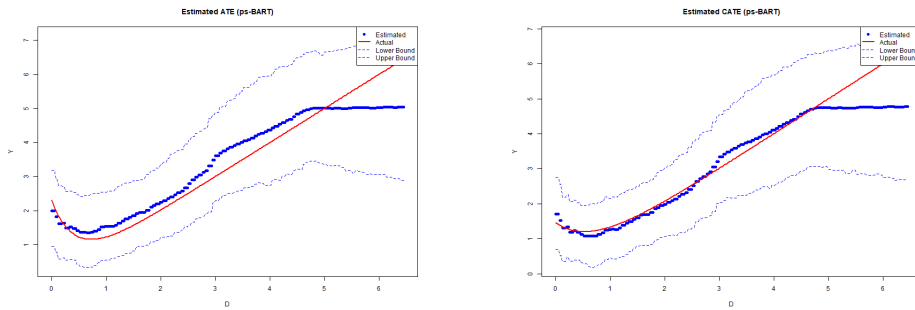


Figure 8: ps-BART ATE and CATE Functions Estimation for $N=100$ (for CATE, an Example of a Random \mathbf{x}_i of a Random Simulation is used)

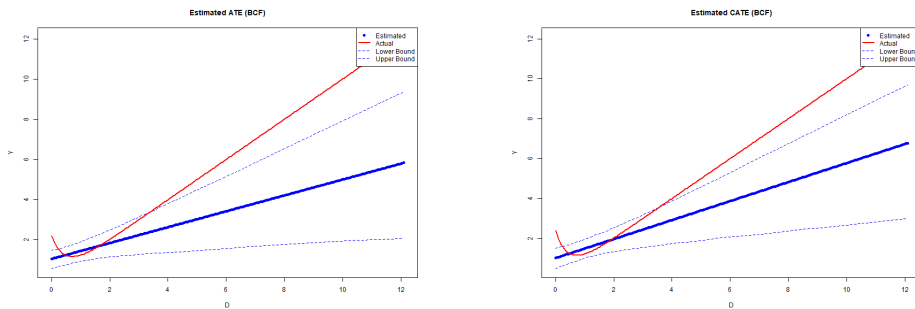


Figure 9: BCF ATE and CATE Functions Estimation for $N=250$ (for CATE, an Example of a Random \mathbf{x}_i of a Random Simulation is used)

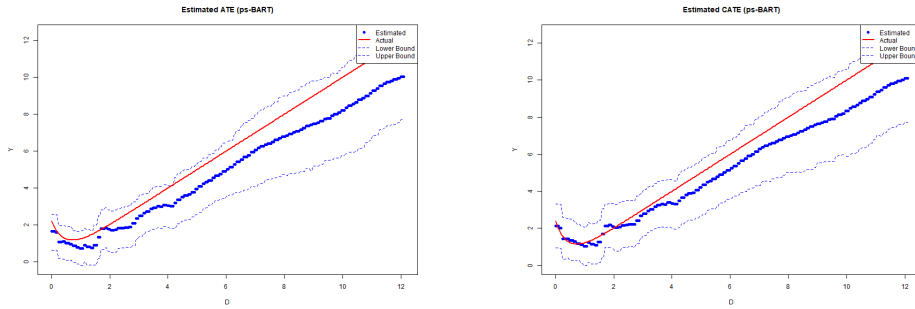


Figure 10: ps-BART ATE and CATE Functions Estimation for $N=250$ (for CATE, an Example of a Random x_i of a Random Simulation is used)

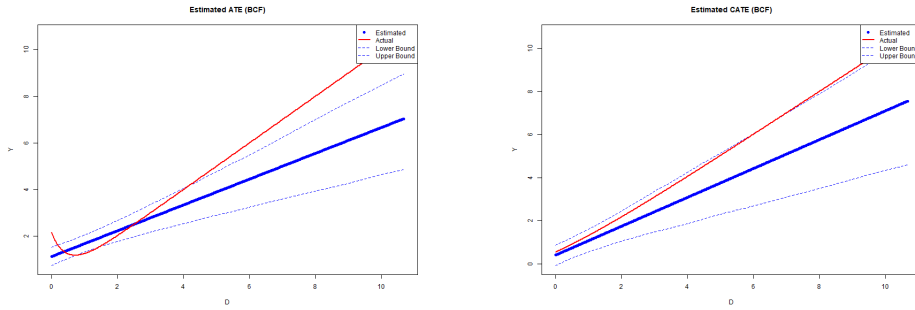


Figure 11: BCF ATE and CATE Functions Estimation for $N=500$ (for CATE, an Example of a Random x_i of a Random Simulation is used)

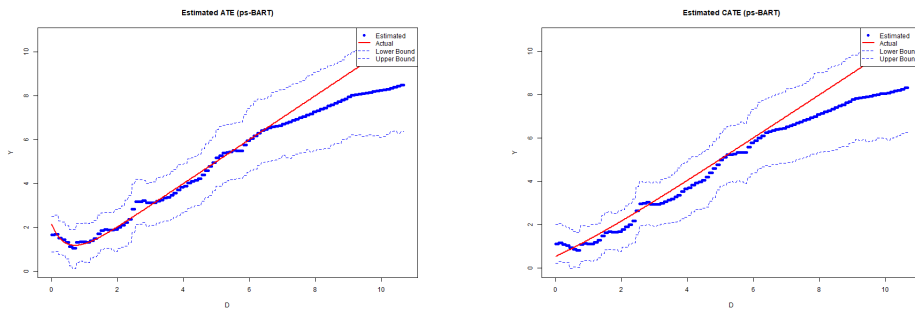


Figure 12: ps-BART ATE and CATE Functions Estimation for $N=500$ (for CATE, an Example of a Random x_i of a Random Simulation is used)

Table 6: Statistical Test Results: p-values for Different Metrics (n=100)

Metric	Fligner-Policello Test	Mann-Whitney U Test	Kruskal-Wallis H Test	Levene's Test	Brown-Forsythe Test
RMSE _{ATE}	1.25×10^{-10}	N/A	N/A	0.0172	0.0567
MAE _{ATE}	6.80×10^{-13}	N/A	N/A	3.52×10^{-5}	0.0046
MAPE _{ATE}	4.63×10^{-10}	N/A	N/A	5.83×10^{-6}	0.00091
Len _{ATE}	0	N/A	N/A	4.73×10^{-5}	9.86×10^{-5}
RMSE _{CATE}	N/A	0.0150	0.0149	0.2229	0.2040
MAE _{CATE}	N/A	0.0148	0.0147	0.1309	0.1315
MAPE _{CATE}	0.1191	N/A	N/A	0.0385	0.0506
Len _{CATE}	0.9269	N/A	N/A	0.0186	0.0656
SEC _{ATE}	1.71×10^{-30}	N/A	N/A	2.13×10^{-7}	2.61×10^{-7}
AEC _{ATE}	1.71×10^{-30}	N/A	N/A	5.51×10^{-13}	1.84×10^{-13}
SEC _{CATE}	0.0482	N/A	N/A	0.00124	0.0734
AEC _{CATE}	0.0482	N/A	N/A	0.00060	0.0702

Table 7: Statistical Test Results: p-values for Different Metrics (n=250)

Metric	Fligner-Policello Test	Mann-Whitney U Test	Kruskal-Wallis H Test	Levene's Test	Brown-Forsythe Test
RMSE _{ATE}	5.88×10^{-31}	N/A	N/A	5.57×10^{-5}	0.00282
MAE _{ATE}	4.99×10^{-22}	N/A	N/A	3.61×10^{-12}	5.03×10^{-7}
MAPE _{ATE}	1.95×10^{-16}	N/A	N/A	1.53×10^{-13}	8.98×10^{-8}
Len _{ATE}	0	N/A	N/A	2.55×10^{-5}	2.54×10^{-5}
RMSE _{CATE}	7.04×10^{-25}	N/A	N/A	2.70×10^{-6}	9.54×10^{-6}
MAE _{CATE}	1.18×10^{-28}	N/A	N/A	1.31×10^{-7}	8.62×10^{-7}
MAPE _{CATE}	2.81×10^{-56}	N/A	N/A	3.45×10^{-8}	9.24×10^{-8}
Len _{CATE}	N/A	0.00363	0.00361	0.2804	0.3984
SEC _{ATE}	0	N/A	N/A	1.34×10^{-26}	1.26×10^{-22}
AEC _{ATE}	0	N/A	N/A	6.41×10^{-22}	2.66×10^{-21}
SEC _{CATE}	3.52×10^{-61}	N/A	N/A	3.88×10^{-31}	2.58×10^{-22}
AEC _{CATE}	3.52×10^{-61}	N/A	N/A	5.61×10^{-27}	2.89×10^{-27}

Table 8: Statistical Test Results: p-values for Different Metrics (n=500)

Metric	Fligner-Policello Test	Mann-Whitney U Test	Kruskal-Wallis H Test	Levene's Test	Brown-Forsythe Test
RMSE _{ATE}	4.81×10^{-112}	N/A	N/A	4.24×10^{-3}	8.76×10^{-3}
MAE _{ATE}	2.56×10^{-41}	N/A	N/A	5.39×10^{-15}	8.01×10^{-12}
MAPE _{ATE}	3.05×10^{-26}	N/A	N/A	2.49×10^{-17}	9.22×10^{-12}
Len _{ATE}	0	N/A	N/A	4.53×10^{-7}	5.31×10^{-7}
RMSE _{CATE}	3.88×10^{-98}	N/A	N/A	8.44×10^{-4}	2.77×10^{-3}
MAE _{CATE}	4.37×10^{-109}	N/A	N/A	2.66×10^{-4}	1.02×10^{-3}
MAPE _{CATE}	0	N/A	N/A	1.98×10^{-4}	1.91×10^{-4}
Len _{CATE}	N/A	8.96×10^{-6}	8.91×10^{-6}	0.2330	0.3937
SEC _{ATE}	0	N/A	N/A	1.31×10^{-37}	1.01×10^{-37}
AEC _{ATE}	0	N/A	N/A	1.68×10^{-32}	4.74×10^{-31}
SEC _{CATE}	0	N/A	N/A	2.19×10^{-27}	2.38×10^{-27}
AEC _{CATE}	0	N/A	N/A	1.05×10^{-18}	1.48×10^{-17}

4.1.3 $\alpha = 4$

The performance measures results for $\alpha = 4$ can be seen in 9. Concerning the point-wise estimation performance metrics, the ps-BART model is clearly superior to the BCF model, albeit the latter still remains more robust for ATE function estimation. Moving to the uncertainty estimation performance measures, it can be concluded that the ps-BART model is significantly better in both ATE and CATE function estimation. Anew, such results were already expected for $\alpha = 4$.

Figures 13, 14, 15, 16, 17, and 18 graphically illustrate the results of Table 9. The misspecification of the BCF model for the underlying DGPs can be visually seen in these figures.

Tables 10, 11, and 12 present the statistical tests results for $n = 100$, $n = 250$, and $n = 500$ respectively. It can be concluded that the ps-BART model is statistically significantly superior to the BCF model, while remaining less robust than the benchmark model for ATE function point-wise estimation (with the exception of $RMSE_{ATE}$).

Table 9: Metric Results

n	Metric	BCF (Mean \pm SD)	ps-BART (Mean \pm SD)
100	RMSE _{ATE}	0.459 \pm 0.111	0.355 \pm 0.139
	MAE _{ATE}	0.351 \pm 0.092	0.276 \pm 0.141
	MAPE _{ATE}	0.207 \pm 0.058	0.169 \pm 0.096
	Len _{ATE}	1.174 \pm 0.218	1.725 \pm 0.230
	Cover _{ATE}	0.804 \pm 0.157	0.977 \pm 0.078
	RMSE _{CATE}	1.054 \pm 0.536	0.831 \pm 0.375
	MAE _{CATE}	0.841 \pm 0.435	0.685 \pm 0.308
	MAPE _{CATE}	0.328 \pm 0.093	0.296 \pm 0.073
	Len _{CATE}	2.440 \pm 0.872	2.574 \pm 0.560
	Cover _{CATE}	0.805 \pm 0.157	0.885 \pm 0.121
	SEC _{ATE}	0.046 \pm 0.058	0.007 \pm 0.032
	AEC _{ATE}	0.169 \pm 0.131	0.057 \pm 0.060
	SEC _{CATE}	0.046 \pm 0.067	0.019 \pm 0.035
	AEC _{CATE}	0.151 \pm 0.152	0.092 \pm 0.102
250	RMSE _{ATE}	0.441 \pm 0.086	0.282 \pm 0.099
	MAE _{ATE}	0.324 \pm 0.053	0.221 \pm 0.101
	MAPE _{ATE}	0.190 \pm 0.027	0.138 \pm 0.067
	Len _{ATE}	0.889 \pm 0.108	1.446 \pm 0.145
	Cover _{ATE}	0.735 \pm 0.128	0.993 \pm 0.021
	RMSE _{CATE}	1.543 \pm 0.652	0.844 \pm 0.322
	MAE _{CATE}	1.233 \pm 0.534	0.685 \pm 0.258
	MAPE _{CATE}	0.380 \pm 0.095	0.249 \pm 0.057
	Len _{CATE}	2.199 \pm 0.602	2.469 \pm 0.440
	Cover _{CATE}	0.528 \pm 0.164	0.880 \pm 0.119
	SEC _{ATE}	0.062 \pm 0.053	0.002 \pm 0.001
	AEC _{ATE}	0.222 \pm 0.115	0.047 \pm 0.009
	SEC _{CATE}	0.205 \pm 0.128	0.019 \pm 0.039
	AEC _{CATE}	0.422 \pm 0.164	0.096 \pm 0.099
500	RMSE _{ATE}	0.456 \pm 0.081	0.255 \pm 0.088
	MAE _{ATE}	0.322 \pm 0.038	0.207 \pm 0.089
	MAPE _{ATE}	0.186 \pm 0.021	0.129 \pm 0.058
	Len _{ATE}	0.719 \pm 0.072	1.293 \pm 0.132
	Cover _{ATE}	0.625 \pm 0.088	0.991 \pm 0.036
	RMSE _{CATE}	2.096 \pm 1.088	0.808 \pm 0.494
	MAE _{CATE}	1.689 \pm 0.911	0.652 \pm 0.401
	MAPE _{CATE}	0.409 \pm 0.080	0.198 \pm 0.043
	Len _{CATE}	2.208 \pm 0.819	2.577 \pm 0.771
	Cover _{CATE}	0.356 \pm 0.110	0.917 \pm 0.084
	SEC _{ATE}	0.113 \pm 0.056	0.003 \pm 0.005
	AEC _{ATE}	0.325 \pm 0.088	0.050 \pm 0.022
	SEC _{CATE}	0.364 \pm 0.117	0.008 \pm 0.018
	AEC _{CATE}	0.594 \pm 0.110	0.063 \pm 0.064

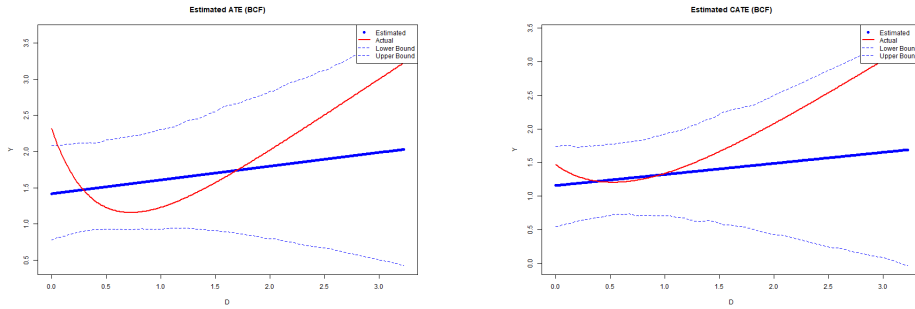


Figure 13: BCF ATE and CATE Functions Estimation for $N=100$ (for CATE, an Example of a Random \mathbf{x}_i of a Random Simulation is used)

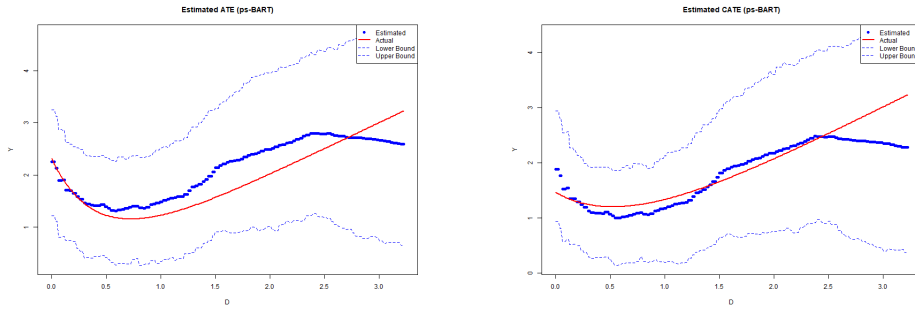


Figure 14: ps-BART ATE and CATE Functions Estimation for $N=100$ (for CATE, an Example of a Random \mathbf{x}_i of a Random Simulation is used)

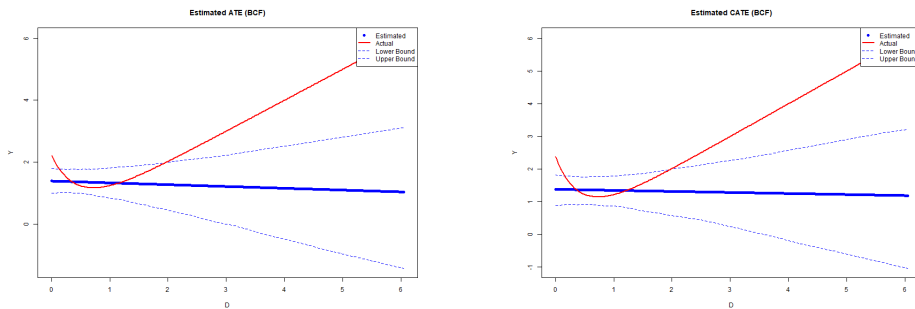


Figure 15: BCF ATE and CATE Functions Estimation for $N=250$ (for CATE, an Example of a Random \mathbf{x}_i of a Random Simulation is used)

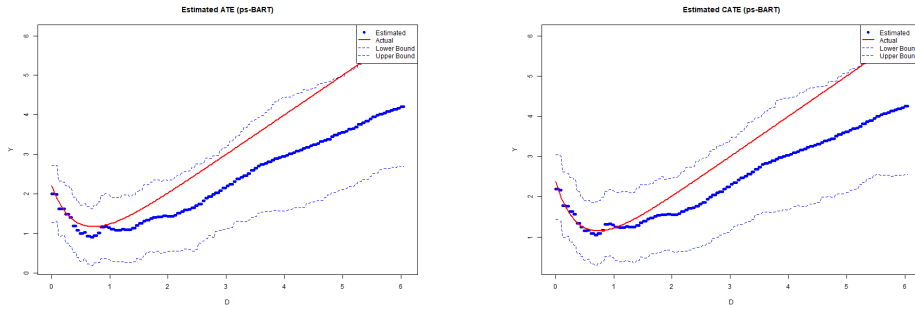


Figure 16: ps-BART ATE and CATE Functions Estimation for $N=250$ (for CATE, an Example of a Random x_i of a Random Simulation is used)

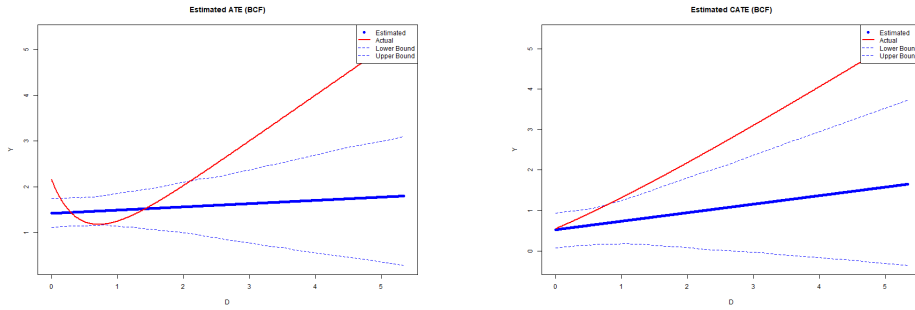


Figure 17: BCF ATE and CATE Functions Estimation for $N=500$ (for CATE, an Example of a Random x_i of a Random Simulation is used)

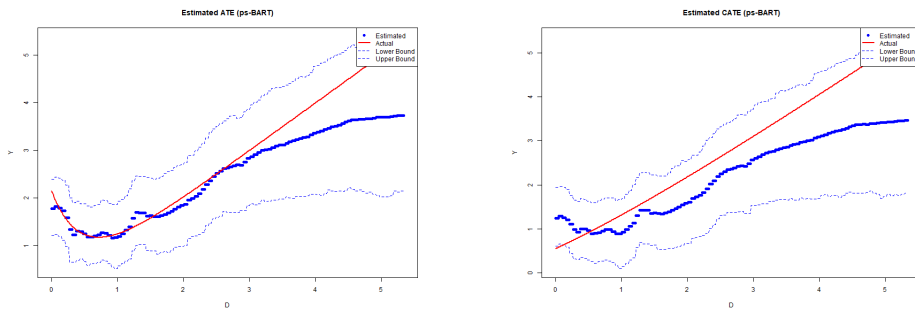


Figure 18: ps-BART ATE and CATE Functions Estimation for $N=500$ (for CATE, an Example of a Random x_i of a Random Simulation is used)

Table 10: Statistical Test Results: p-values for Different Metrics (n=100)

Metric	Fligner-Policello Test	Mann-Whitney U Test	Kruskal-Wallis H Test	Levene's Test	Brown-Forsythe Test
RMSE _{ATE}	N/A	1.91×10^{-12}	1.90×10^{-12}	0.5227	0.7332
MAE _{ATE}	N/A	2.94×10^{-11}	2.91×10^{-11}	0.1015	0.2298
MAPE _{ATE}	2.15×10^{-12}	N/A	N/A	0.0104	0.0655
Len _{ATE}	N/A	2.12×10^{-29}	2.09×10^{-29}	0.3127	0.3397
RMSE _{CATE}	N/A	2.89×10^{-4}	2.88×10^{-4}	0.0650	0.1165
MAE _{CATE}	N/A	2.56×10^{-3}	2.55×10^{-3}	0.0883	0.1377
MAPE _{CATE}	0.0171	N/A	N/A	0.0132	0.0199
Len _{CATE}	0.0024	N/A	N/A	0.0015	0.0125
SEC _{ATE}	1.82×10^{-10}	N/A	N/A	1.26×10^{-11}	4.07×10^{-9}
AEC _{ATE}	1.82×10^{-10}	N/A	N/A	8.89×10^{-19}	5.13×10^{-19}
SEC _{CATE}	0.3268	N/A	N/A	1.10×10^{-6}	1.82×10^{-4}
AEC _{CATE}	0.3268	N/A	N/A	1.44×10^{-7}	2.53×10^{-6}

Table 11: Statistical Test Results: p-values for Different Metrics (n=250)

Metric	Fligner-Policello Test	Mann-Whitney U Test	Kruskal-Wallis H Test	Levene's Test	Brown-Forsythe Test
RMSE _{ATE}	N/A	1.64×10^{-20}	1.62×10^{-20}	0.1460	0.2392
MAE _{ATE}	2.12×10^{-21}	N/A	N/A	4.38×10^{-8}	1.18×10^{-5}
MAPE _{ATE}	1.45×10^{-14}	N/A	N/A	1.62×10^{-12}	2.69×10^{-8}
Len _{ATE}	0	N/A	N/A	0.0097	0.0114
RMSE _{CATE}	1.21×10^{-42}	N/A	N/A	6.22×10^{-6}	3.74×10^{-5}
MAE _{CATE}	2.57×10^{-38}	N/A	N/A	4.59×10^{-6}	2.89×10^{-5}
MAPE _{CATE}	1.76×10^{-63}	N/A	N/A	7.88×10^{-5}	1.74×10^{-4}
Len _{CATE}	1.26×10^{-6}	N/A	N/A	0.0055	0.0138
SEC _{ATE}	1.40×10^{-42}	N/A	N/A	1.15×10^{-31}	1.81×10^{-24}
AEC _{ATE}	1.40×10^{-42}	N/A	N/A	1.50×10^{-30}	1.52×10^{-30}
SEC _{CATE}	9.87×10^{-115}	N/A	N/A	6.10×10^{-21}	1.69×10^{-20}
AEC _{CATE}	9.87×10^{-115}	N/A	N/A	8.48×10^{-6}	4.74×10^{-6}

Table 12: Statistical Test Results: p-values for Different Metrics (n=500)

Metric	Fligner-Policello Test	Mann-Whitney U Test	Kruskal-Wallis H Test	Levene's Test	Brown-Forsythe Test
RMSE _{ATE}	N/A	1.64×10^{-20}	1.62×10^{-20}	0.1460	0.2392
MAE _{ATE}	2.12×10^{-21}	N/A	N/A	4.38×10^{-8}	1.18×10^{-5}
MAPE _{ATE}	1.45×10^{-14}	N/A	N/A	1.62×10^{-12}	2.69×10^{-8}
Len _{ATE}	0	N/A	N/A	0.0097	0.0114
RMSE _{CATE}	1.21×10^{-42}	N/A	N/A	6.22×10^{-6}	3.74×10^{-5}
MAE _{CATE}	2.57×10^{-38}	N/A	N/A	4.59×10^{-6}	2.89×10^{-5}
MAPE _{CATE}	1.76×10^{-63}	N/A	N/A	7.88×10^{-5}	1.74×10^{-4}
Len _{CATE}	1.26×10^{-6}	N/A	N/A	0.0055	0.0138
SEC _{ATE}	1.40×10^{-42}	N/A	N/A	1.15×10^{-31}	1.81×10^{-24}
AEC _{ATE}	1.40×10^{-42}	N/A	N/A	1.50×10^{-30}	1.52×10^{-30}
SEC _{CATE}	9.87×10^{-115}	N/A	N/A	6.10×10^{-21}	1.69×10^{-20}
AEC _{CATE}	9.87×10^{-115}	N/A	N/A	8.48×10^{-6}	4.74×10^{-6}

4.1.4 $\alpha = 8$

The results for $\alpha = 4$ are presented in 13. Regarding the point-wise estimation performance measures, the ps-BART model is still superior to the BCF model, though to a less extent considering ATE function estimation and BCF remaining more robust for ATE function estimation. Moving to the uncertainty estimation performance metrics, it can be concluded that the ps-BART model is superior in both ATE and CATE function estimation. Interestingly the jump from 4 to 8 for the α value had a more negative impact on the relative performance of the ps-BART model than the BCF model for ATE function estimation, showing a limitation of the proposed model for highly nonlinear relationships between the treatment and the outcome.

Figures 19, 20, 21, 22, 23, and 24 graphically illustrate the results of Table 13. The misspecification of the BCF model for the underlying DGPs can be visually seen in these figures.

Tables 14, 15, and 16 show the statistical tests results for $n = 100$, $n = 250$, and $n = 500$ respectively. It can be seen that the proposed model is statistically significantly superior to the BCF model, while remaining less robust than the benchmark model for ATE function point-wise estimation for $n = 250$ and $n = 500$.

Table 13: Metric Results

n	Metric	BCF (Mean \pm SD)	ps-BART (Mean \pm SD)
100	RMSE _{ATE}	0.352 \pm 0.118	0.301 \pm 0.158
	MAE _{ATE}	0.278 \pm 0.115	0.257 \pm 0.163
	MAPE _{ATE}	0.166 \pm 0.070	0.160 \pm 0.102
	Len _{ATE}	1.248 \pm 0.251	1.670 \pm 0.196
	Cover _{ATE}	0.906 \pm 0.161	0.984 \pm 0.073
	RMSE _{CATE}	0.859 \pm 0.371	0.638 \pm 0.234
	MAE _{CATE}	0.694 \pm 0.299	0.546 \pm 0.204
	MAPE _{CATE}	0.440 \pm 0.125	0.381 \pm 0.101
	Len _{CATE}	2.021 \pm 0.537	2.451 \pm 0.352
	Cover _{CATE}	0.795 \pm 0.130	0.940 \pm 0.088
	SEC _{ATE}	0.028 \pm 0.060	0.006 \pm 0.030
	AEC _{ATE}	0.106 \pm 0.129	0.058 \pm 0.055
	SEC _{CATE}	0.041 \pm 0.050	0.008 \pm 0.033
	AEC _{CATE}	0.157 \pm 0.128	0.047 \pm 0.075
250	RMSE _{ATE}	0.327 \pm 0.090	0.259 \pm 0.116
	MAE _{ATE}	0.226 \pm 0.081	0.216 \pm 0.118
	MAPE _{ATE}	0.134 \pm 0.045	0.136 \pm 0.073
	Len _{ATE}	0.935 \pm 0.111	1.411 \pm 0.139
	Cover _{ATE}	0.905 \pm 0.148	0.991 \pm 0.034
	RMSE _{CATE}	1.344 \pm 0.487	0.706 \pm 0.214
	MAE _{CATE}	1.076 \pm 0.393	0.611 \pm 0.187
	MAPE _{CATE}	0.575 \pm 0.139	0.375 \pm 0.084
	Len _{CATE}	1.764 \pm 0.384	2.334 \pm 0.300
	Cover _{CATE}	0.501 \pm 0.128	0.904 \pm 0.109
	SEC _{ATE}	0.024 \pm 0.055	0.003 \pm 0.004
	AEC _{ATE}	0.093 \pm 0.124	0.050 \pm 0.018
	SEC _{CATE}	0.218 \pm 0.109	0.014 \pm 0.039
	AEC _{CATE}	0.449 \pm 0.128	0.070 \pm 0.095
500	RMSE _{ATE}	0.341 \pm 0.079	0.233 \pm 0.093
	MAE _{ATE}	0.224 \pm 0.061	0.198 \pm 0.096
	MAPE _{ATE}	0.130 \pm 0.034	0.124 \pm 0.060
	Len _{ATE}	0.775 \pm 0.078	1.218 \pm 0.100
	Cover _{ATE}	0.865 \pm 0.144	0.992 \pm 0.036
	RMSE _{CATE}	1.883 \pm 0.871	0.700 \pm 0.337
	MAE _{CATE}	1.514 \pm 0.720	0.605 \pm 0.286
	MAPE _{CATE}	0.662 \pm 0.121	0.319 \pm 0.070
	Len _{CATE}	1.736 \pm 0.563	2.293 \pm 0.334
	Cover _{CATE}	0.336 \pm 0.081	0.892 \pm 0.110
	SEC _{ATE}	0.028 \pm 0.050	0.003 \pm 0.005
	AEC _{ATE}	0.114 \pm 0.122	0.051 \pm 0.020
	SEC _{CATE}	0.383 \pm 0.096	0.015 \pm 0.038
	AEC _{CATE}	0.614 \pm 0.081	0.080 \pm 0.095

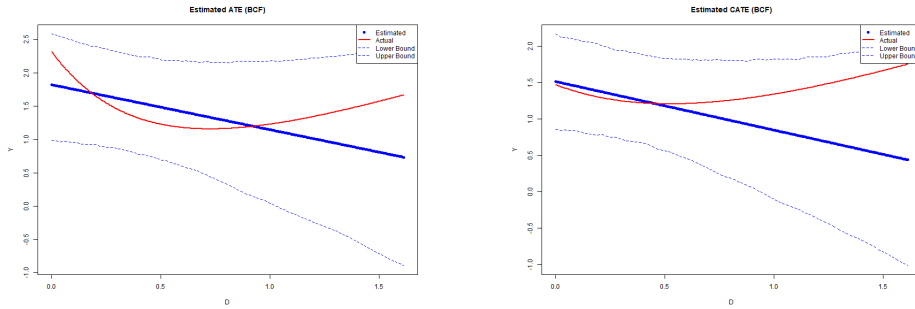


Figure 19: BCF ATE and CATE Functions Estimation for $N=100$ (for CATE, an Example of a Random \mathbf{x}_i of a Random Simulation is used)

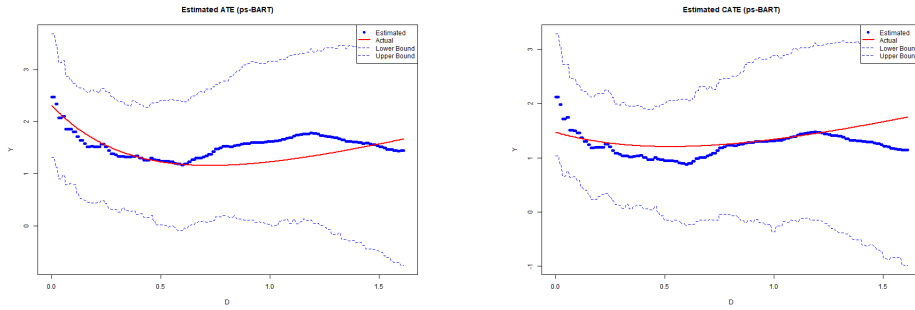


Figure 20: ps-BART ATE and CATE Functions Estimation for $N=100$ (for CATE, an Example of a Random \mathbf{x}_i of a Random Simulation is used)

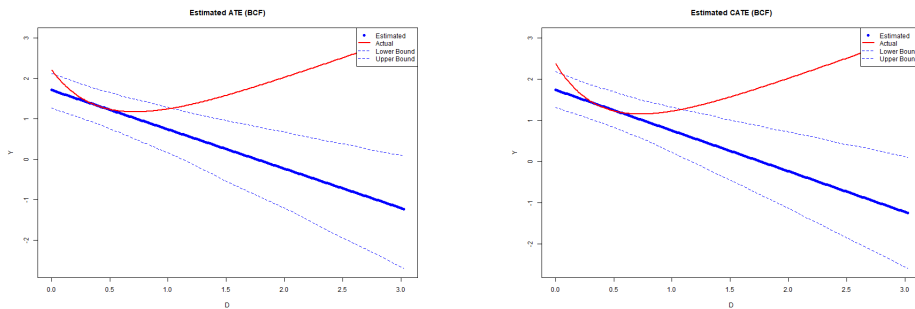


Figure 21: BCF ATE and CATE Functions Estimation for $N=250$ (for CATE, an Example of a Random \mathbf{x}_i of a Random Simulation is used)

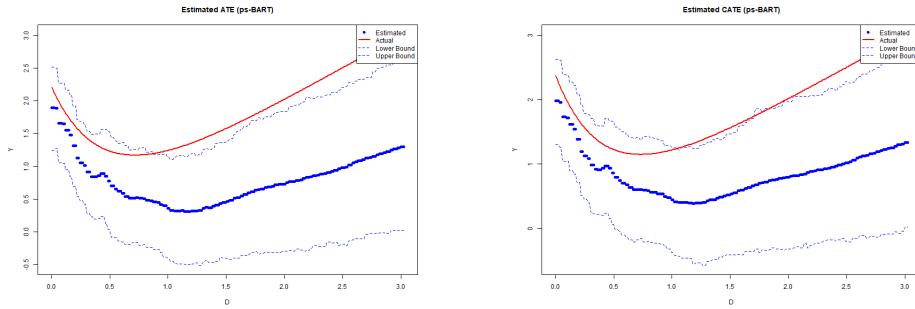


Figure 22: ps-BART ATE and CATE Functions Estimation for $N=250$ (for CATE, an Example of a Random x_i of a Random Simulation is used)

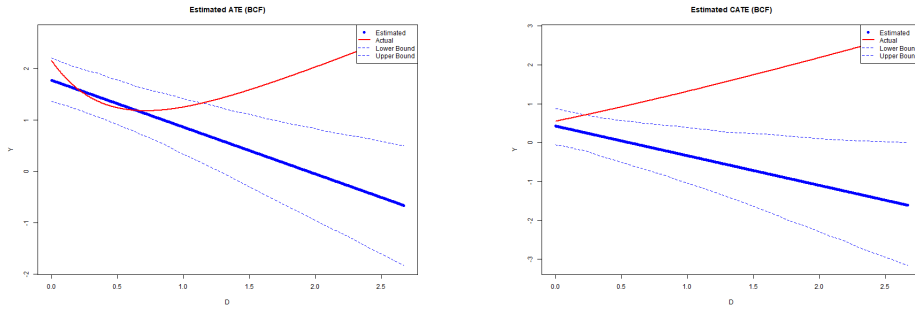


Figure 23: BCF ATE and CATE Functions Estimation for $N=500$ (for CATE, an Example of a Random x_i of a Random Simulation is used)

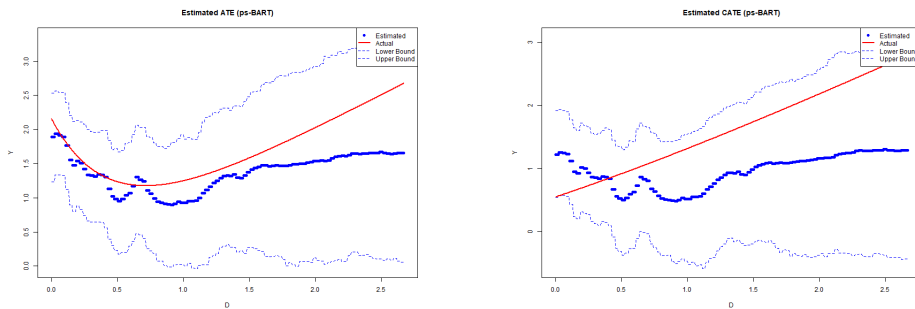


Figure 24: ps-BART ATE and CATE Functions Estimation for $N=500$ (for CATE, an Example of a Random x_i of a Random Simulation is used)

Table 14: Statistical Test Results: p-values for Different Metrics (n=100)

Metric	Fligner-Policello Test	Mann-Whitney U Test	Kruskal-Wallis H Test	Levene's Test	Brown-Forsythe Test
RMSE _{ATE}	N/A	2.38×10^{-5}	2.37×10^{-5}	0.2042	0.3304
MAE _{ATE}	N/A	9.63×10^{-3}	9.60×10^{-3}	0.1057	0.1838
MAPE _{ATE}	5.02×10^{-2}	N/A	N/A	0.0340	0.0635
Len _{ATE}	4.92×10^{-85}	N/A	N/A	0.0468	0.0493
RMSE _{CATE}	8.85×10^{-9}	N/A	N/A	7.06×10^{-4}	2.28×10^{-3}
MAE _{CATE}	1.54×10^{-5}	N/A	N/A	4.50×10^{-3}	6.48×10^{-3}
MAPE _{CATE}	3.57×10^{-4}	N/A	N/A	1.15×10^{-2}	1.18×10^{-2}
Len _{CATE}	1.34×10^{-18}	N/A	N/A	0.0110	0.0295
SEC _{ATE}	2.24×10^{-1}	N/A	N/A	8.77×10^{-9}	1.19×10^{-3}
AEC _{ATE}	2.24×10^{-1}	N/A	N/A	5.48×10^{-14}	2.55×10^{-5}
SEC _{CATE}	1.53×10^{-10}	N/A	N/A	8.75×10^{-9}	1.78×10^{-8}
AEC _{CATE}	1.53×10^{-10}	N/A	N/A	6.05×10^{-14}	6.80×10^{-15}

Table 15: Statistical Test Results: p-values for Different Metrics (n=250)

Metric	Fligner-Policello Test	Mann-Whitney U Test	Kruskal-Wallis H Test	Levene's Test	Brown-Forsythe Test
RMSE _{ATE}	6.46×10^{-9}	N/A	N/A	0.0375	0.0656
MAE _{ATE}	0.0485	N/A	N/A	0.0011	0.0066
MAPE _{ATE}	0.3220	N/A	N/A	0.00015	0.00058
Len _{ATE}	0	N/A	N/A	0.0391	0.0472
RMSE _{CATE}	2.88×10^{-99}	N/A	N/A	7.55×10^{-8}	1.25×10^{-7}
MAE _{CATE}	5.44×10^{-61}	N/A	N/A	8.83×10^{-7}	1.24×10^{-6}
MAPE _{CATE}	7.59×10^{-73}	N/A	N/A	1.83×10^{-5}	2.07×10^{-5}
Len _{CATE}	6.06×10^{-47}	N/A	N/A	0.0423	0.1053
SEC _{ATE}	4.75×10^{-6}	N/A	N/A	2.77×10^{-14}	5.75×10^{-5}
AEC _{ATE}	4.75×10^{-6}	N/A	N/A	9.30×10^{-20}	2.94×10^{-7}
SEC _{CATE}	0	N/A	N/A	1.83×10^{-19}	1.91×10^{-20}
AEC _{CATE}	0	N/A	N/A	2.70×10^{-4}	1.63×10^{-5}

Table 16: Statistical Test Results: p-values for Different Metrics (n=500)

Metric	Fligner-Policello Test	Mann-Whitney U Test	Kruskal-Wallis H Test	Levene's Test	Brown-Forsythe Test
RMSE _{ATE}	7.83×10^{-25}	N/A	N/A	0.0460	0.0711
MAE _{ATE}	0.00114	N/A	N/A	8.02×10^{-5}	3.79×10^{-4}
MAPE _{ATE}	0.0354	N/A	N/A	5.38×10^{-7}	7.41×10^{-6}
Len _{ATE}	0	N/A	N/A	0.0296	0.0291
RMSE _{CATE}	2.46×10^{-306}	N/A	N/A	2.17×10^{-6}	4.89×10^{-5}
MAE _{CATE}	1.33×10^{-243}	N/A	N/A	6.25×10^{-6}	1.18×10^{-4}
MAPE _{CATE}	0	N/A	N/A	4.06×10^{-4}	3.89×10^{-4}
Len _{CATE}	5.42×10^{-36}	N/A	N/A	1.64×10^{-3}	7.47×10^{-3}
SEC _{ATE}	0.5357	N/A	N/A	3.68×10^{-18}	3.19×10^{-7}
AEC _{ATE}	0.5357	N/A	N/A	4.25×10^{-27}	9.43×10^{-12}
SEC _{CATE}	0	N/A	N/A	9.01×10^{-13}	5.98×10^{-14}
AEC _{CATE}	N/A	3.90×10^{-34}	3.84×10^{-34}	0.2891	0.9279

4.1.5 Conclusion

It can be concluded that based on the results of the 1st set of DGPs, the proposed model is statistically significantly better at ATE and CATE functions estimation than the benchmark model, considering both dimensions of point-wise and uncertainty estimation. Even when the degree of nonlinearity is not substantial, the ps-BART model is statistically significantly superior for $n \geq 250$. Finally, it can also be concluded that the BCF model is seemingly statistically significantly more robust than the proposed model for ATE function estimation in the domain of point-wise estimation. Besides this last result, the results of this 1st set of DGPs were already expected given the misspecification of the BCF model for the considered DGPs.

4.2 2nd Set of DGPs

4.2.1 Specification 1

Table 17 presents the performance metrics results for the 2nd Set of DGPs with Specification 1. It can be seen that the ps-BART model becomes clearly superior in both point-wise estimation and uncertainty estimation, while also being more robust than the BCF model for ATE function point-wise estimation this time. The superiority of the ps-BART model is confirmed (i.e., shown to be statistically significant) by the results of the statistical tests found in Tables 18, 19, and 20. Interestingly, the uncertainty estimation performance for CATE function estimation of the proposed model considerably decreased when $n = 500$ due to the fact that the model was overconfident.

Figures 25, 26, 27, 28, 29, and 30 graphically illustrate the results of Table 17. The misspecification of the BCF model can be visually seen even more clearly for this DGP.

Table 17: Metric Results

n	Metric	BCF (Mean \pm SD)	ps-BART (Mean \pm SD)
100	RMSE _{ATE}	99 \pm 27	20 \pm 9
	MAE _{ATE}	51 \pm 12	10 \pm 5
	MAPE _{ATE}	7 \pm 8	2 \pm 3
	Len _{ATE}	101 \pm 29	133 \pm 37
	Cover _{ATE}	0.722 \pm 0.179	0.991 \pm 0.006
	RMSE _{CATE}	205 \pm 89	36 \pm 22
	MAE _{CATE}	131 \pm 55	21 \pm 12
	MAPE _{CATE}	8 \pm 11	2 \pm 1
	Len _{CATE}	142 \pm 35	159 \pm 61
	Cover _{CATE}	0.536 \pm 0.060	0.970 \pm 0.032
	SEC _{ATE}	0.084 \pm 0.129	0.002 \pm 0.000
	AEC _{ATE}	0.229 \pm 0.179	0.041 \pm 0.006
	SEC _{CATE}	0.175 \pm 0.049	0.001 \pm 0.002
	AEC _{CATE}	0.414 \pm 0.061	0.033 \pm 0.018
250	RMSE _{ATE}	105 \pm 26	8 \pm 7
	MAE _{ATE}	52 \pm 11	4 \pm 1
	MAPE _{ATE}	6 \pm 8	1 \pm 3
	Len _{ATE}	79 \pm 17	29 \pm 7
	Cover _{ATE}	0.601 \pm 0.187	0.991 \pm 0.008
	RMSE _{CATE}	304 \pm 134	26 \pm 32
	MAE _{CATE}	192 \pm 84	15 \pm 15
	MAPE _{CATE}	7 \pm 3	1 \pm 4
	Len _{CATE}	133 \pm 26	85 \pm 56
	Cover _{CATE}	0.446 \pm 0.045	0.974 \pm 0.022
	SEC _{ATE}	0.157 \pm 0.153	0.002 \pm 0.001
	AEC _{ATE}	0.349 \pm 0.187	0.041 \pm 0.008
	SEC _{CATE}	0.256 \pm 0.046	0.001 \pm 0.001
	AEC _{CATE}	0.504 \pm 0.045	0.030 \pm 0.013
500	RMSE _{ATE}	103 \pm 17	5 \pm 3
	MAE _{ATE}	51 \pm 7	3 \pm 1
	MAPE _{ATE}	6 \pm 4	0.3 \pm 0.2
	Len _{ATE}	69 \pm 17	14 \pm 2
	Cover _{ATE}	0.510 \pm 0.181	0.938 \pm 0.029
	RMSE _{CATE}	346 \pm 105	21 \pm 15
	MAE _{CATE}	216 \pm 65	12 \pm 7
	MAPE _{CATE}	7 \pm 4	1 \pm 0.3
	Len _{CATE}	128 \pm 19	57 \pm 30
	Cover _{CATE}	0.402 \pm 0.038	0.887 \pm 0.029
	SEC _{ATE}	0.226 \pm 0.152	0.001 \pm 0.002
	AEC _{ATE}	0.440 \pm 0.181	0.023 \pm 0.022
	SEC _{CATE}	0.302 \pm 0.041	0.005 \pm 0.006
	AEC _{CATE}	0.548 \pm 0.038	0.063 \pm 0.029

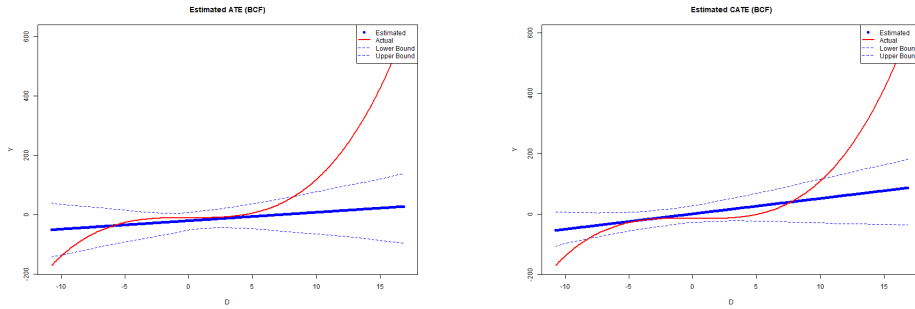


Figure 25: BCF ATE and CATE Functions Estimation for $N=100$ (for CATE, an Example of a Random \mathbf{x}_i of a Random Simulation is used)

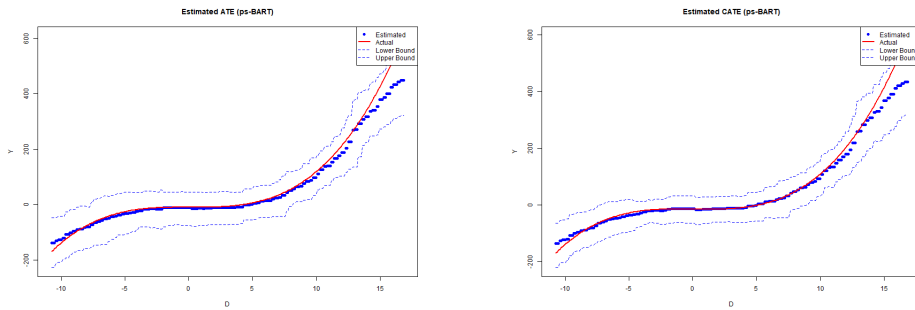


Figure 26: ps-BART ATE and CATE Functions Estimation for $N=100$ (for CATE, an Example of a Random \mathbf{x}_i of a Random Simulation is used)

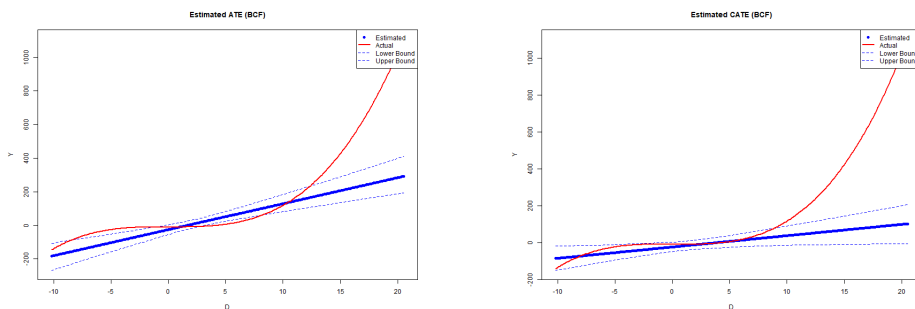


Figure 27: BCF ATE and CATE Functions Estimation for $N=250$ (for CATE, an Example of a Random \mathbf{x}_i of a Random Simulation is used)

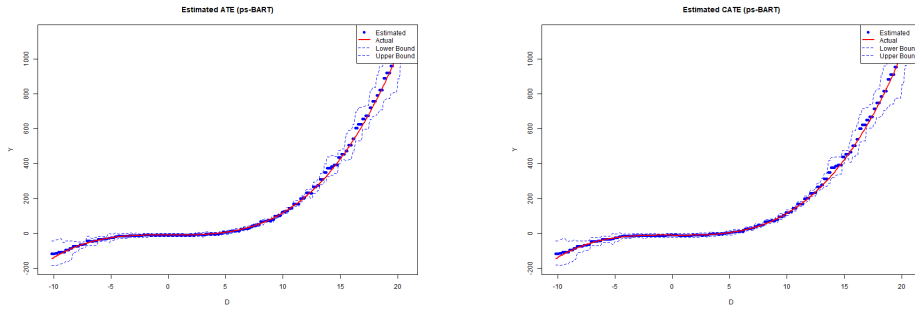


Figure 28: ps-BART ATE and CATE Functions Estimation for $N=250$ (for CATE, an Example of a Random x_i of a Random Simulation is used)

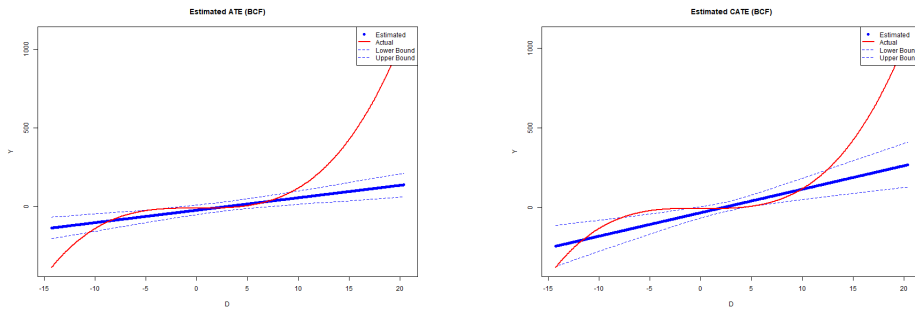


Figure 29: BCF ATE and CATE Functions Estimation for $N=500$ (for CATE, an Example of a Random x_i of a Random Simulation is used)

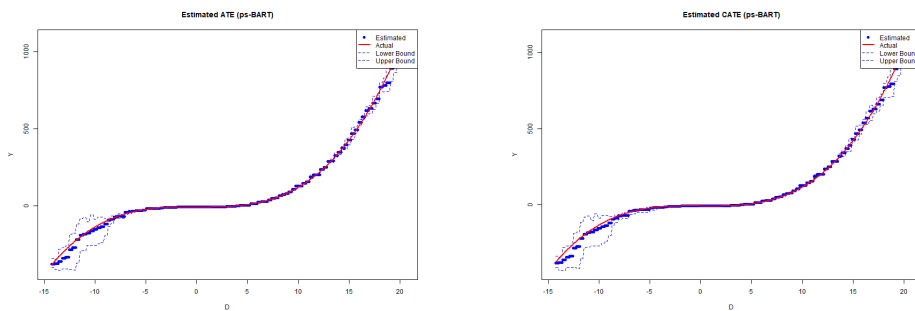


Figure 30: ps-BART ATE and CATE Functions Estimation for $N=500$ (for CATE, an Example of a Random x_i of a Random Simulation is used)

Table 18: Statistical Test Results: p-values for Different Metrics (n=100)

Metric	Fligner-Policello Test	Mann-Whitney U Test	Kruskal-Wallis H Test	Levene's Test	Brown-Forsythe Test
RMSE _{ATE}	0	N/A	N/A	1.62×10^{-13}	5.11×10^{-13}
MAE _{ATE}	0	N/A	N/A	3.28×10^{-10}	8.74×10^{-9}
MAPE _{ATE}	6.60×10^{-37}	N/A	N/A	1.99×10^{-6}	9.98×10^{-4}
Len _{ATE}	2.51×10^{-14}	N/A	N/A	0.0476	0.0567
RMSE _{CATE}	0	N/A	N/A	1.85×10^{-15}	7.56×10^{-15}
MAE _{CATE}	0	N/A	N/A	7.64×10^{-17}	6.08×10^{-16}
MAPE _{CATE}	0	N/A	N/A	5.72×10^{-3}	0.0414
Len _{CATE}	0.0824	N/A	N/A	4.09×10^{-4}	1.32×10^{-3}
SEC _{ATE}	7.56×10^{-54}	N/A	N/A	7.15×10^{-17}	1.28×10^{-8}
AEC _{ATE}	7.56×10^{-54}	N/A	N/A	5.26×10^{-23}	2.67×10^{-17}
SEC _{CATE}	0	N/A	N/A	7.16×10^{-34}	7.15×10^{-34}
AEC _{CATE}	0	N/A	N/A	1.82×10^{-19}	9.39×10^{-19}

Table 19: Statistical Test Results: p-values for Different Metrics (n=250)

Metric	Fligner-Policello Test	Mann-Whitney U Test	Kruskal-Wallis H Test	Levene's Test	Brown-Forsythe Test
RMSE _{ATE}	0	N/A	N/A	1.18×10^{-19}	1.01×10^{-18}
MAE _{ATE}	0	N/A	N/A	8.31×10^{-18}	1.23×10^{-13}
MAPE _{ATE}	1.07×10^{-126}	N/A	N/A	2.70×10^{-6}	4.79×10^{-5}
Len _{ATE}	0	N/A	N/A	3.77×10^{-11}	8.76×10^{-10}
RMSE _{CATE}	0	N/A	N/A	2.03×10^{-15}	1.51×10^{-12}
MAE _{CATE}	0	N/A	N/A	6.12×10^{-17}	1.24×10^{-13}
MAPE _{CATE}	N/A	2.46×10^{-30}	2.43×10^{-30}	0.1452	0.0545
Len _{CATE}	1.90×10^{-40}	N/A	N/A	0.0043	0.0391
SEC _{ATE}	0	N/A	N/A	1.68×10^{-35}	1.11×10^{-15}
AEC _{ATE}	0	N/A	N/A	1.52×10^{-37}	1.86×10^{-22}
SEC _{CATE}	0	N/A	N/A	6.75×10^{-30}	4.25×10^{-27}
AEC _{CATE}	0	N/A	N/A	1.83×10^{-18}	1.96×10^{-17}

Table 20: Statistical Test Results: p-values for Different Metrics (n=500)

Metric	Fligner-Policello Test	Mann-Whitney U Test	Kruskal-Wallis H Test	Levene's Test	Brown-Forsythe Test
RMSE _{ATE}	0	N/A	N/A	3.52×10^{-26}	3.20×10^{-26}
MAE _{ATE}	0	N/A	N/A	3.35×10^{-22}	5.99×10^{-21}
MAPE _{ATE}	0	N/A	N/A	4.42×10^{-21}	1.40×10^{-18}
Len _{ATE}	0	N/A	N/A	4.33×10^{-12}	9.71×10^{-11}
RMSE _{CATE}	0	N/A	N/A	3.98×10^{-19}	1.02×10^{-17}
MAE _{CATE}	0	N/A	N/A	6.96×10^{-20}	2.97×10^{-18}
MAPE _{CATE}	0	N/A	N/A	1.47×10^{-10}	2.23×10^{-8}
Len _{CATE}	N/A	9.45×10^{-30}	9.32×10^{-30}	0.0734	0.197
SEC _{ATE}	0	N/A	N/A	8.74×10^{-45}	8.80×10^{-45}
AEC _{ATE}	0	N/A	N/A	1.85×10^{-38}	8.05×10^{-33}
SEC _{CATE}	0	N/A	N/A	1.98×10^{-21}	1.66×10^{-21}
AEC _{CATE}	0	N/A	N/A	0.0170	0.0132

4.2.2 Specification 2

The performance measures results for Specification 2 can be found in Table 21. Based on the results, it can be inferred that the ps-BART model is superior in both point-wise estimation and uncertainty estimation, while also being more robust than the benchmark model. The superiority of the ps-BART model is also statistically significant based on the results of the statistical tests found in Tables 22, 23, and 24. Interestingly, the uncertainty estimation performance for both the ATE and CATE functions estimation of the proposed model considerably decreased when $n = 500$, which could mean that the model decreases the confidence interval length to a faster rate than it should when n tends to infinity.

Figures 31, 32, 33, 34, 35, and 36 graphically illustrate the results of Table 21. The misspecification of the benchmark model can be clearly seen in the figures.

Table 21: Metric Results

<i>n</i>	Metric	BCF (Mean \pm SD)	ps-BART (Mean \pm SD)
100	RMSE _{ATE}	276 \pm 69	92 \pm 39
	MAE _{ATE}	150 \pm 32	53 \pm 21
	MAPE _{ATE}	14 \pm 56	3 \pm 12
	Len _{ATE}	406 \pm 72	424 \pm 118
	Cover _{ATE}	0.801 \pm 0.076	0.986 \pm 0.010
	RMSE _{CATE}	485 \pm 208	171 \pm 99
	MAE _{CATE}	337 \pm 122	117 \pm 61
	MAPE _{CATE}	56 \pm 92	16 \pm 24
	Len _{CATE}	456 \pm 96	532 \pm 184
	Cover _{CATE}	0.510 \pm 0.060	0.940 \pm 0.045
	SEC _{ATE}	0.028 \pm 0.033	0.001 \pm 0.001
	AEC _{ATE}	0.149 \pm 0.076	0.036 \pm 0.009
	SEC _{CATE}	0.197 \pm 0.051	0.002 \pm 0.002
	AEC _{CATE}	0.440 \pm 0.060	0.038 \pm 0.025
250	RMSE _{ATE}	281 \pm 94	30 \pm 21
	MAE _{ATE}	147 \pm 32	18 \pm 16
	MAPE _{ATE}	10 \pm 17	0.4 \pm 0.5
	Len _{ATE}	297 \pm 70	106 \pm 40
	Cover _{ATE}	0.719 \pm 0.111	0.952 \pm 0.152
	RMSE _{CATE}	736 \pm 588	78 \pm 81
	MAE _{CATE}	486 \pm 351	46 \pm 46
	MAPE _{CATE}	78 \pm 178	3 \pm 3
	Len _{CATE}	352 \pm 74	275 \pm 246
	Cover _{CATE}	0.377 \pm 0.043	0.967 \pm 0.033
	SEC _{ATE}	0.066 \pm 0.084	0.023 \pm 0.125
	AEC _{ATE}	0.231 \pm 0.111	0.055 \pm 0.142
	SEC _{CATE}	0.331 \pm 0.050	0.001 \pm 0.004
	AEC _{CATE}	0.573 \pm 0.043	0.030 \pm 0.022
500	RMSE _{ATE}	272 \pm 68	19 \pm 13
	MAE _{ATE}	143 \pm 27	10 \pm 3
	MAPE _{ATE}	17 \pm 66	0.2 \pm 0.5
	Len _{ATE}	227 \pm 47	44 \pm 21
	Cover _{ATE}	0.656 \pm 0.124	0.863 \pm 0.050
	RMSE _{CATE}	864 \pm 606	73 \pm 108
	MAE _{CATE}	563 \pm 362	40 \pm 59
	MAPE _{CATE}	79 \pm 111	2 \pm 2
	Len _{CATE}	318 \pm 56	192 \pm 196
	Cover _{CATE}	0.344 \pm 0.040	0.884 \pm 0.038
	SEC _{ATE}	0.102 \pm 0.094	0.010 \pm 0.010
	AEC _{ATE}	0.294 \pm 0.124	0.090 \pm 0.046
	SEC _{CATE}	0.369 \pm 0.050	0.006 \pm 0.008
	AEC _{CATE}	0.606 \pm 0.040	0.066 \pm 0.038

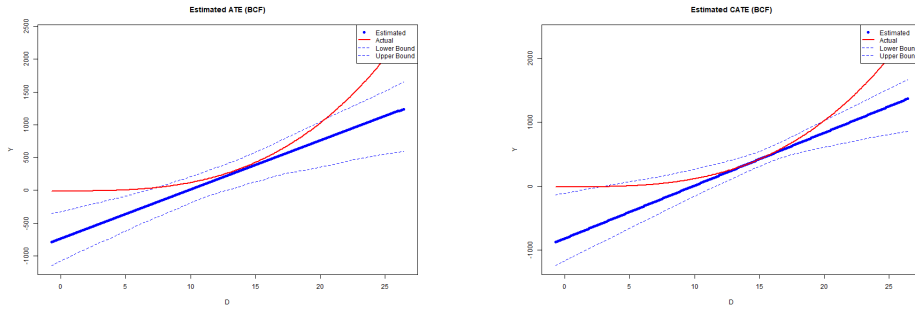


Figure 31: BCF ATE and CATE Functions Estimation for $N=100$ (for CATE, an Example of a Random \mathbf{x}_i of a Random Simulation is used)

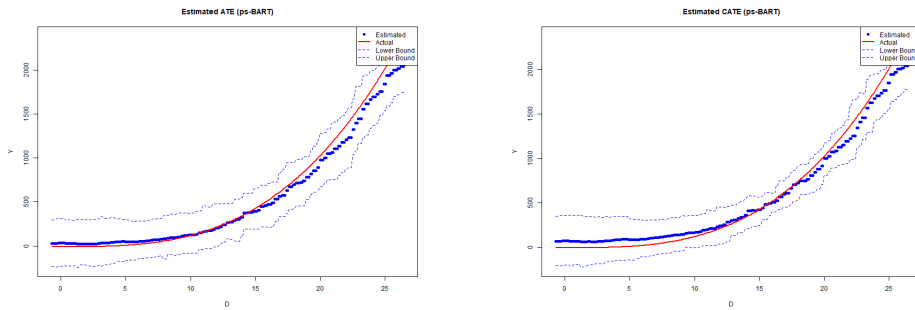


Figure 32: ps-BART ATE and CATE Functions Estimation for $N=100$ (for CATE, an Example of a Random \mathbf{x}_i of a Random Simulation is used)

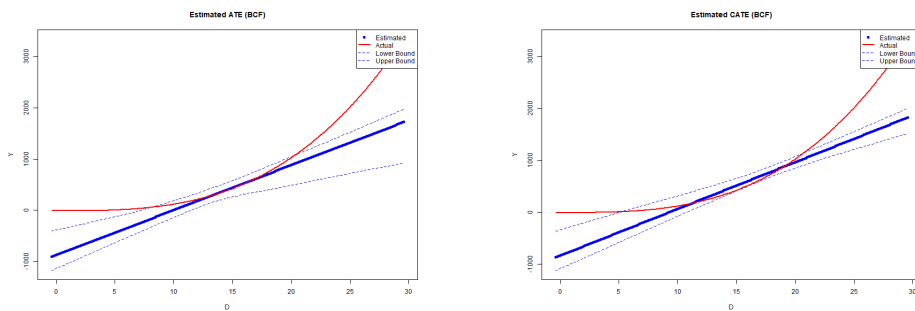


Figure 33: BCF ATE and CATE Functions Estimation for $N=250$ (for CATE, an Example of a Random \mathbf{x}_i of a Random Simulation is used)

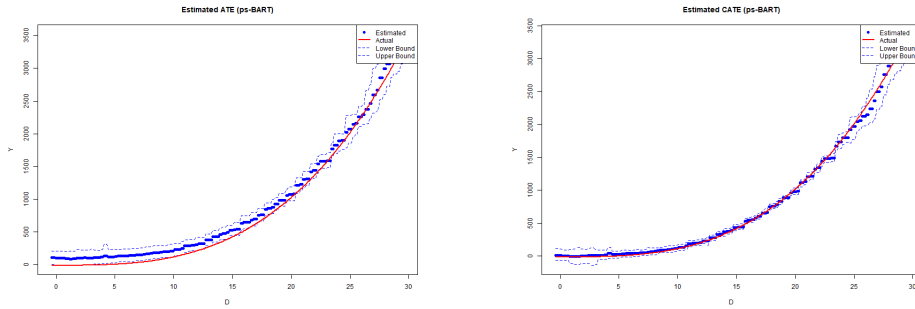


Figure 34: ps-BART ATE and CATE Functions Estimation for $N=250$ (for CATE, an Example of a Random x_i of a Random Simulation is used)

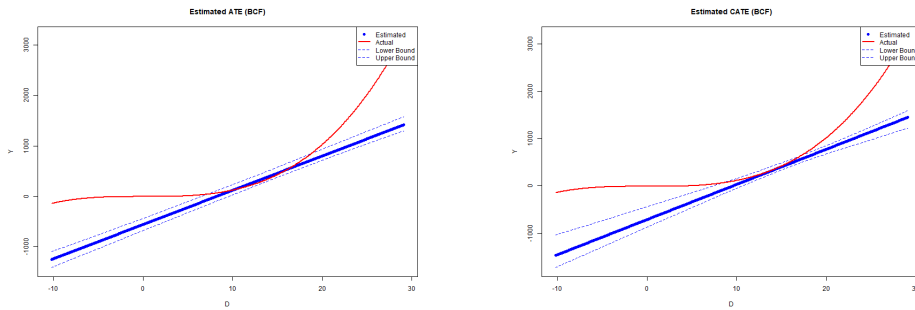


Figure 35: BCF ATE and CATE Functions Estimation for $N=500$ (for CATE, an Example of a Random x_i of a Random Simulation is used)

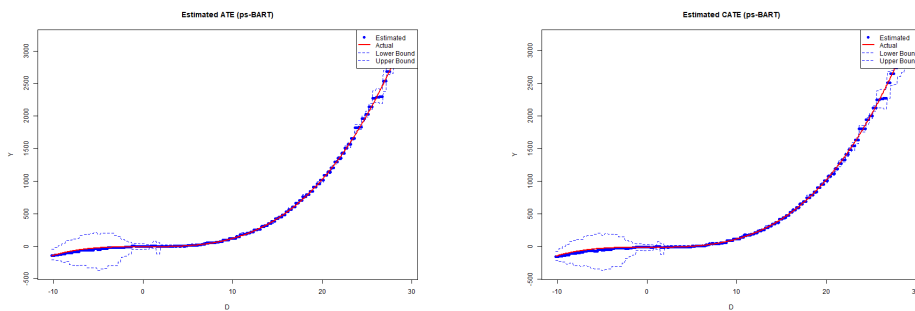


Figure 36: ps-BART ATE and CATE Functions Estimation for $N=500$ (for CATE, an Example of a Random x_i of a Random Simulation is used)

Table 22: Statistical Test Results: p-values for Different Metrics (n=100)

Metric	Fligner-Policello Test	Mann-Whitney U Test	Kruskal-Wallis H Test	Levene's Test	Brown-Forsythe Test
RMSE _{ATE}	0	N/A	N/A	2.85×10^{-5}	2.16×10^{-5}
MAE _{ATE}	0	N/A	N/A	3.39×10^{-5}	7.76×10^{-5}
MAPE _{ATE}	9.20×10^{-67}	N/A	N/A	0.0228	0.1352
Len _{ATE}	0.8339	N/A	N/A	6.13×10^{-4}	0.00453
RMSE _{CATE}	2.37×10^{-258}	N/A	N/A	1.76×10^{-6}	1.16×10^{-4}
MAE _{CATE}	0	N/A	N/A	6.15×10^{-6}	2.38×10^{-4}
MAPE _{CATE}	4.20×10^{-105}	N/A	N/A	0.0146	0.0378
Len _{CATE}	0.00227	N/A	N/A	7.97×10^{-5}	0.00290
SEC _{ATE}	1.22×10^{-174}	N/A	N/A	4.48×10^{-12}	2.45×10^{-9}
AEC _{ATE}	1.22×10^{-174}	N/A	N/A	9.66×10^{-18}	3.47×10^{-17}
SEC _{CATE}	0	N/A	N/A	5.22×10^{-26}	4.87×10^{-26}
AEC _{CATE}	0	N/A	N/A	4.01×10^{-10}	7.95×10^{-10}

Table 23: Statistical Test Results: p-values for Different Metrics (n=250)

Metric	Fligner-Policello Test	Mann-Whitney U Test	Kruskal-Wallis H Test	Levene's Test	Brown-Forsythe Test
RMSE _{ATE}	0	N/A	N/A	3.76×10^{-7}	8.95×10^{-7}
MAE _{ATE}	0	N/A	N/A	3.10×10^{-9}	2.40×10^{-8}
MAPE _{ATE}	0	N/A	N/A	1.64×10^{-6}	3.62×10^{-4}
Len _{ATE}	0	N/A	N/A	9.29×10^{-5}	8.68×10^{-5}
RMSE _{CATE}	0	N/A	N/A	1.98×10^{-8}	8.03×10^{-6}
MAE _{CATE}	0	N/A	N/A	2.24×10^{-8}	7.61×10^{-6}
MAPE _{CATE}	0	N/A	N/A	0.00147	0.0217
Len _{CATE}	9.93×10^{-22}	N/A	N/A	9.85×10^{-4}	0.0163
SEC _{ATE}	N/A	1.46×10^{-30}	1.44×10^{-30}	0.9278	0.2347
AEC _{ATE}	N/A	1.46×10^{-30}	1.44×10^{-30}	0.0566	0.0154
SEC _{CATE}	0	N/A	N/A	2.17×10^{-28}	3.20×10^{-27}
AEC _{CATE}	0	N/A	N/A	9.08×10^{-12}	1.28×10^{-11}

Table 24: Statistical Test Results: p-values for Different Metrics (n=500)

Metric	Fligner-Policello Test	Mann-Whitney U Test	Kruskal-Wallis H Test	Levene's Test	Brown-Forsythe Test
RMSE _{ATE}	0	N/A	N/A	2.01×10^{-14}	1.76×10^{-11}
MAE _{ATE}	0	N/A	N/A	2.13×10^{-15}	6.70×10^{-12}
MAPE _{ATE}	0	N/A	N/A	0.00815	0.0625
Len _{ATE}	0	N/A	N/A	2.96×10^{-14}	9.60×10^{-14}
RMSE _{CATE}	0	N/A	N/A	8.65×10^{-11}	1.16×10^{-6}
MAE _{CATE}	0	N/A	N/A	7.10×10^{-11}	7.80×10^{-7}
MAPE _{CATE}	0	N/A	N/A	6.76×10^{-5}	0.00175
Len _{CATE}	1.35×10^{-31}	N/A	N/A	1.67×10^{-6}	0.00268
SEC _{ATE}	0	N/A	N/A	3.38×10^{-15}	4.39×10^{-10}
AEC _{ATE}	0	N/A	N/A	7.40×10^{-11}	8.15×10^{-9}
SEC _{CATE}	0	N/A	N/A	1.90×10^{-23}	2.47×10^{-22}
AEC _{CATE}	N/A	2.56×10^{-34}	2.52×10^{-34}	0.1751	0.1873

4.2.3 Specification 3

Table 25 shows the results for Specification 3. Based on these results, it can be easily seen that the ps-BART model is superior in both point-wise estimation and uncertainty estimation, while also being more robust than the benchmark model. The superiority of the proposed model is also statistically significant based on the results of the statistical tests found in Tables 22, 23, and 24. Interestingly, the uncertainty estimation performance for both the ATE and CATE functions estimation of the proposed model considerably decreased when compared to Specification 1 and 2. It could be theorized that this is due to the addition of the $3\sqrt{2}C_3^2$ in the determination of the treatment value, which increases the complexity and nonlinearity of the problem.

Figures 37, 38, 39, 40, 41, and 42 graphically illustrate the results of Table 25. The misspecification of the BCF model and the poor uncertainty estimation performance of the proposed model can be clearly seen in the figures.

Table 25: Metric Results

<i>n</i>	Metric	BCF (Mean \pm SD)	ps-BART (Mean \pm SD)
100	RMSE _{ATE}	1410 \pm 793	805 \pm 411
	MAE _{ATE}	473 \pm 156	407 \pm 159
	MAPE _{ATE}	17 \pm 63	7 \pm 24
	Len _{ATE}	1021 \pm 363	1845 \pm 1041
	Cover _{ATE}	0.844 \pm 0.066	0.921 \pm 0.067
	RMSE _{CATE}	3471 \pm 2689	1849 \pm 1315
	MAE _{CATE}	2167 \pm 1653	1307 \pm 903
	MAPE _{CATE}	64 \pm 138	47 \pm 36
	Len _{CATE}	1765 \pm 914	2961 \pm 2105
	Cover _{CATE}	0.474 \pm 0.065	0.707 \pm 0.109
	SEC _{ATE}	0.015 \pm 0.018	0.005 \pm 0.012
	AEC _{ATE}	0.106 \pm 0.065	0.049 \pm 0.054
	SEC _{CATE}	0.231 \pm 0.062	0.071 \pm 0.056
	AEC _{CATE}	0.476 \pm 0.065	0.243 \pm 0.109
250	RMSE _{ATE}	1727 \pm 798	546 \pm 321
	MAE _{ATE}	495 \pm 109	198 \pm 101
	MAPE _{ATE}	9 \pm 15	3 \pm 5
	Len _{ATE}	717 \pm 270	390 \pm 142
	Cover _{ATE}	0.760 \pm 0.081	0.703 \pm 0.150
	RMSE _{CATE}	6508 \pm 4667	1867 \pm 1398
	MAE _{CATE}	4080 \pm 2923	1187 \pm 836
	MAPE _{CATE}	57 \pm 104	25 \pm 41
	Len _{CATE}	1642 \pm 968	2344 \pm 2665
	Cover _{CATE}	0.335 \pm 0.043	0.536 \pm 0.143
	SEC _{ATE}	0.043 \pm 0.031	0.083 \pm 0.108
	AEC _{ATE}	0.190 \pm 0.080	0.247 \pm 0.149
	SEC _{CATE}	0.380 \pm 0.052	0.192 \pm 0.122
	AEC _{CATE}	0.615 \pm 0.043	0.414 \pm 0.143
500	RMSE _{ATE}	1933 \pm 605	425 \pm 271
	MAE _{ATE}	510 \pm 87	97 \pm 56
	MAPE _{ATE}	4 \pm 4	1 \pm 2
	Len _{ATE}	476 \pm 125	192 \pm 80
	Cover _{ATE}	0.661 \pm 0.053	0.801 \pm 0.057
	RMSE _{CATE}	9549 \pm 4961	1974 \pm 1475
	MAE _{CATE}	6059 \pm 3162	1184 \pm 934
	MAPE _{CATE}	44 \pm 30	11 \pm 10
	Len _{CATE}	1406 \pm 486	2325 \pm 1908
	Cover _{CATE}	0.247 \pm 0.023	0.594 \pm 0.137
	SEC _{ATE}	0.086 \pm 0.031	0.025 \pm 0.017
	AEC _{ATE}	0.289 \pm 0.053	0.149 \pm 0.057
	SEC _{CATE}	0.494 \pm 0.033	0.145 \pm 0.104
	AEC _{CATE}	0.703 \pm 0.023	0.356 \pm 0.137

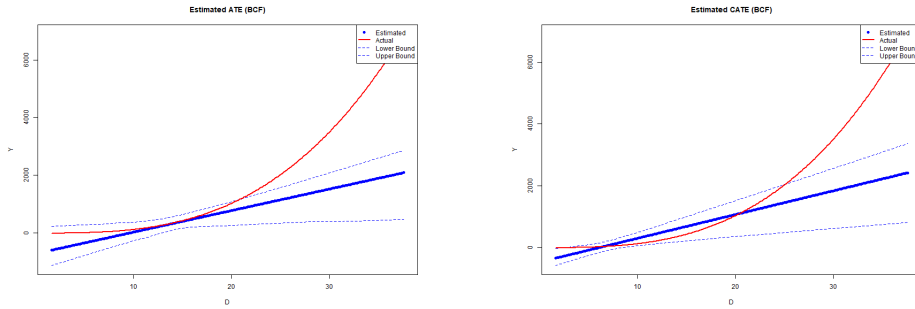


Figure 37: BCF ATE and CATE Functions Estimation for $N=100$ (for CATE, an Example of a Random \mathbf{x}_i of a Random Simulation is used)

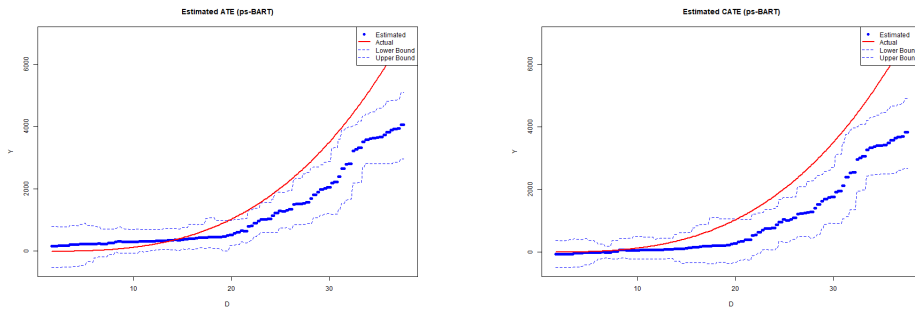


Figure 38: ps-BART ATE and CATE Functions Estimation for $N=100$ (for CATE, an Example of a Random \mathbf{x}_i of a Random Simulation is used)

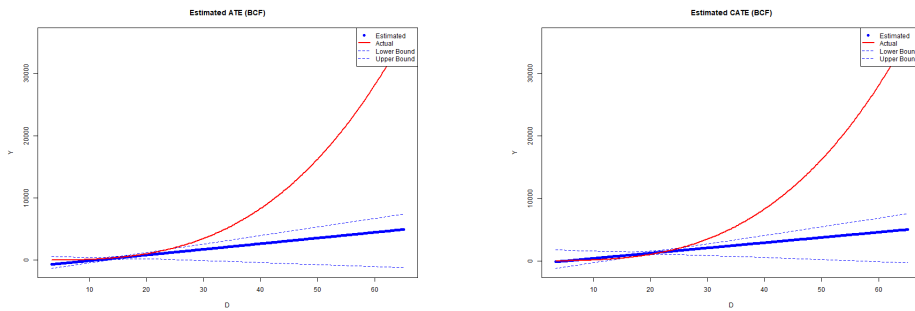


Figure 39: BCF ATE and CATE Functions Estimation for $N=250$ (for CATE, an Example of a Random \mathbf{x}_i of a Random Simulation is used)

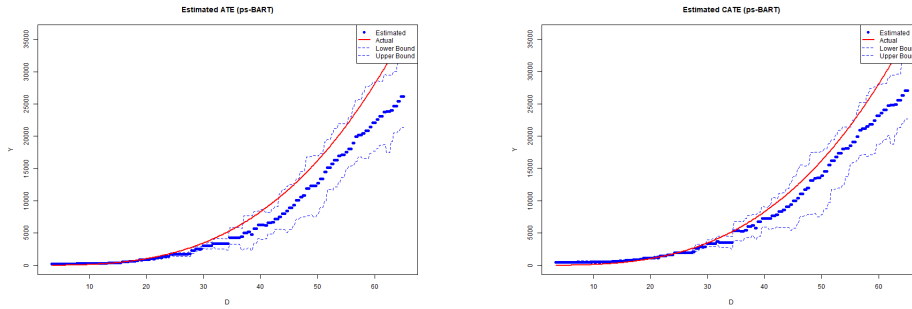


Figure 40: ps-BART ATE and CATE Functions Estimation for $N=250$ (for CATE, an Example of a Random x_i of a Random Simulation is used)

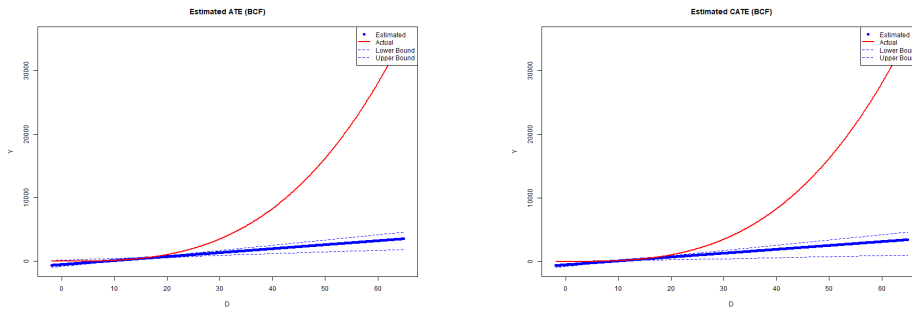


Figure 41: BCF ATE and CATE Functions Estimation for $N=500$ (for CATE, an Example of a Random x_i of a Random Simulation is used)

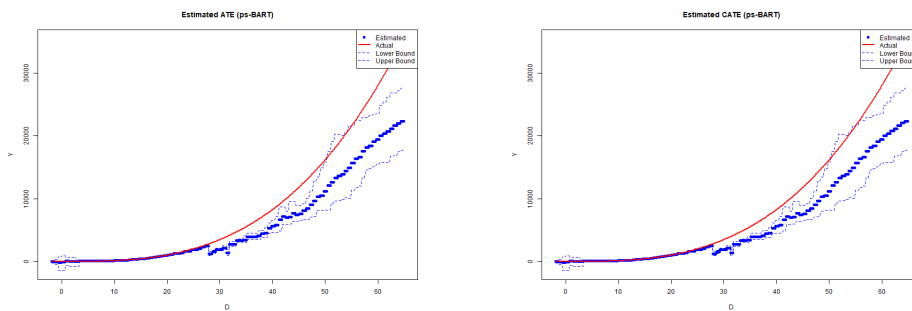


Figure 42: ps-BART ATE and CATE Functions Estimation for $N=500$ (for CATE, an Example of a Random x_i of a Random Simulation is used)

Table 26: Statistical Test Results: p-values for Different Metrics (n=100)

Metric	Fligner-Policello Test	Mann-Whitney U Test	Kruskal-Wallis H Test	Levene's Test	Brown-Forsythe Test
RMSE _{ATE}	6.77×10^{-31}	N/A	N/A	4.65×10^{-4}	0.00342
MAE _{ATE}	N/A	4.82×10^{-4}	4.80×10^{-4}	0.9608	0.9225
MAPE _{ATE}	N/A	4.23×10^{-6}	4.21×10^{-6}	0.0638	0.2209
Len _{ATE}	7.81×10^{-35}	N/A	N/A	4.89×10^{-7}	6.22×10^{-6}
RMSE _{CATE}	1.46×10^{-20}	N/A	N/A	4.29×10^{-4}	0.00344
MAE _{CATE}	3.04×10^{-13}	N/A	N/A	0.00201	0.0112
MAPE _{CATE}	N/A	0.2742	0.2737	0.0856	0.2845
Len _{CATE}	1.63×10^{-14}	N/A	N/A	7.51×10^{-5}	0.00148
SEC _{ATE}	3.84×10^{-18}	N/A	N/A	1.10×10^{-4}	3.16×10^{-4}
AEC _{ATE}	3.84×10^{-18}	N/A	N/A	0.00193	0.00135
SEC _{CATE}	N/A	4.76×10^{-30}	4.70×10^{-30}	0.2349	0.2413
AEC _{CATE}	0	N/A	N/A	2.31×10^{-6}	2.83×10^{-6}

Table 27: Statistical Test Results: p-values for Different Metrics (n=250)

Metric	Fligner-Policello Test	Mann-Whitney U Test	Kruskal-Wallis H Test	Levene's Test	Brown-Forsythe Test
RMSE _{ATE}	0	N/A	N/A	1.86×10^{-5}	1.16×10^{-4}
MAE _{ATE}	N/A	3.57×10^{-31}	3.52×10^{-31}	0.1515	0.1177
MAPE _{ATE}	6.24×10^{-16}	N/A	N/A	4.44×10^{-4}	0.00717
Len _{ATE}	7.35×10^{-82}	N/A	N/A	4.23×10^{-4}	0.00118
RMSE _{CATE}	1.12×10^{-185}	N/A	N/A	8.62×10^{-7}	1.21×10^{-5}
MAE _{CATE}	4.05×10^{-191}	N/A	N/A	8.01×10^{-7}	1.29×10^{-5}
MAPE _{CATE}	2.73×10^{-43}	N/A	N/A	0.0138	0.1046
Len _{CATE}	0.0154	N/A	N/A	0.00295	0.0236
SEC _{ATE}	0.00839	N/A	N/A	3.87×10^{-6}	1.06×10^{-4}
AEC _{ATE}	0.00839	N/A	N/A	9.78×10^{-7}	2.49×10^{-6}
SEC _{CATE}	1.08×10^{-65}	N/A	N/A	1.04×10^{-15}	1.98×10^{-12}
AEC _{CATE}	1.08×10^{-65}	N/A	N/A	1.47×10^{-22}	3.30×10^{-22}

Table 28: Statistical Test Results: p-values for Different Metrics (n=500)

Metric	Fligner-Policello Test	Mann-Whitney U Test	Kruskal-Wallis H Test	Levene's Test	Brown-Forsythe Test
RMSE _{ATE}	0	N/A	N/A	1.01×10^{-7}	8.87×10^{-7}
MAE _{ATE}	0	N/A	N/A	3.38×10^{-5}	2.52×10^{-5}
MAPE _{ATE}	5.76×10^{-137}	N/A	N/A	3.15×10^{-7}	2.38×10^{-5}
Len _{ATE}	0	N/A	N/A	1.35×10^{-5}	9.55×10^{-5}
RMSE _{CATE}	0	N/A	N/A	3.34×10^{-14}	1.99×10^{-10}
MAE _{CATE}	0	N/A	N/A	2.49×10^{-14}	1.48×10^{-10}
MAPE _{CATE}	5.89×10^{-172}	N/A	N/A	2.12×10^{-6}	1.41×10^{-4}
Len _{CATE}	0.00255	N/A	N/A	1.30×10^{-12}	9.37×10^{-8}
SEC _{ATE}	0	N/A	N/A	1.53×10^{-7}	2.00×10^{-7}
AEC _{ATE} *	N/A	N/A	N/A	N/A	N/A
SEC _{CATE}	0	N/A	N/A	2.37×10^{-18}	2.48×10^{-12}
AEC _{CATE}	0	N/A	N/A	5.77×10^{-27}	8.28×10^{-24}

*: AEC_{ATE} had p-values of 1.45×10^{-43} for the T-test and 0.55 for the F-test

4.2.4 Conclusion

In conclusion, it can be affirmed that the ps-BART model is clearly superior to the BCF model for considerably nonlinear DGPs in both point-wise and uncertainty estimation of the ATE and CATE functions. Additionally, for this set of DGPs, the proposed model is more robust than the benchmark model, contradicting the results (and respective conclusion) of the first set of DGPs. Such contradiction could be possibly explained by proposing that for significantly nonlinear DGPs the ps-BART model becomes more robust than the BCF model due to the considerably misspecification of the latter while for slightly nonlinear/considerably linear DGPs, the benchmark model is more robust. Yet, to confirm or disprove this possible explanation, the results of the 3rd set of DGPs are needed.

4.3 3rd Set of DGPs

4.3.1 Linear Relationship

Table 29 presents the results of all metrics for the 3rd Set of DGPs with Linear Relationship. Considering the point-wise estimation performance metrics, both models have a similar performance and robustness for ATE function estimation while the benchmark model being superior and more robust for CATE function estimation. Moving to the uncertainty estimation performance measures, it can be seen that the ps-BART model is considerably better in ATE function estimation and slightly better in CATE function estimation, albeit also having a considerably poor performance for CATE function estimation.

Figures 43, 44, 45, 46, 47, and 48 graphically illustrate the results of Table 29. The correct specification of the BCF model for the underlying DGP, which leads to its advantage over the proposed nonparametric model, can be visually seen in these figures.

The statistical tests results for $n = 100$, $n = 250$, and $n = 500$ can be seen in Tables 30, 31, and 32 respectively. For $n = 100$, it can be concluded (based on the results) that the similarity of both models in point-wise estimation performance for ATE function estimation is statistically significant while the superiority and greater robustness of the benchmark model is statistically significant for CATE function estimation. Moving to uncertainty estimation, it can be seen that the ps-BART model is statistically significantly better than the BCF model for ATE function estimation, while for CATE function estimation, it cannot be said that the two models possess a different performance.

Moving to $n = 250$ and $n = 500$, the aforementioned conclusions remain true, apart from the affirmation that it cannot be said that the two models possess a different uncertainty estimation performance for CATE function estimation as now the ps-BART model is statistically significantly superior (though its performance is considerably poor).

Table 29: Metric Results

<i>n</i>	Metric	BCF (Mean \pm SD)	ps-BART (Mean \pm SD)
100	RMSE _{ATE}	2.838 \pm 0.878	3.061 \pm 0.868
	MAE _{ATE}	2.751 \pm 0.873	2.785 \pm 0.800
	MAPE _{ATE}	1.050 \pm 0.386	1.045 \pm 0.409
	Len _{ATE}	8.550 \pm 1.529	13.272 \pm 4.629
	Cover _{ATE}	0.847 \pm 0.307	0.989 \pm 0.025
	RMSE _{CATE}	4.582 \pm 0.827	6.785 \pm 3.619
	MAE _{CATE}	4.339 \pm 0.720	5.843 \pm 2.629
	MAPE _{CATE}	4.397 \pm 3.362	4.707 \pm 3.394
	Len _{CATE}	8.022 \pm 3.551	8.496 \pm 3.783
	Cover _{CATE}	0.468 \pm 0.102	0.442 \pm 0.095
	SEC _{ATE}	0.104 \pm 0.238	0.002 \pm 0.001
	AEC _{ATE}	0.179 \pm 0.269	0.044 \pm 0.014
	SEC _{CATE}	0.243 \pm 0.097	0.267 \pm 0.097
	AEC _{CATE}	0.482 \pm 0.102	0.508 \pm 0.095
250	RMSE _{ATE}	3.049 \pm 0.787	3.136 \pm 0.908
	MAE _{ATE}	2.953 \pm 0.765	2.973 \pm 0.891
	MAPE _{ATE}	1.080 \pm 0.273	1.088 \pm 0.390
	Len _{ATE}	6.004 \pm 1.319	13.730 \pm 3.432
	Cover _{ATE}	0.444 \pm 0.397	0.994 \pm 0.015
	RMSE _{CATE}	4.263 \pm 0.509	7.146 \pm 3.565
	MAE _{CATE}	4.104 \pm 0.433	5.995 \pm 2.400
	MAPE _{CATE}	3.576 \pm 2.335	4.130 \pm 2.591
	Len _{CATE}	4.618 \pm 1.783	8.033 \pm 3.589
	Cover _{CATE}	0.285 \pm 0.076	0.375 \pm 0.066
	SEC _{ATE}	0.412 \pm 0.364	0.002 \pm 0.001
	AEC _{ATE}	0.530 \pm 0.365	0.046 \pm 0.007
	SEC _{CATE}	0.448 \pm 0.098	0.335 \pm 0.077
	AEC _{CATE}	0.665 \pm 0.076	0.575 \pm 0.066
500	RMSE _{ATE}	3.169 \pm 1.142	3.126 \pm 0.923
	MAE _{ATE}	3.051 \pm 1.093	3.017 \pm 0.941
	MAPE _{ATE}	1.082 \pm 0.360	1.070 \pm 0.333
	Len _{ATE}	3.995 \pm 0.823	13.270 \pm 3.759
	Cover _{ATE}	0.173 \pm 0.281	0.983 \pm 0.105
	RMSE _{CATE}	4.015 \pm 0.228	7.304 \pm 2.547
	MAE _{CATE}	3.914 \pm 0.195	6.067 \pm 1.709
	MAPE _{CATE}	3.335 \pm 2.015	3.697 \pm 2.062
	Len _{CATE}	3.022 \pm 0.869	7.507 \pm 2.988
	Cover _{CATE}	0.200 \pm 0.054	0.319 \pm 0.074
	SEC _{ATE}	0.683 \pm 0.302	0.012 \pm 0.085
	AEC _{ATE}	0.784 \pm 0.264	0.058 \pm 0.093
	SEC _{CATE}	0.566 \pm 0.081	0.403 \pm 0.091
	AEC _{CATE}	0.750 \pm 0.054	0.631 \pm 0.074

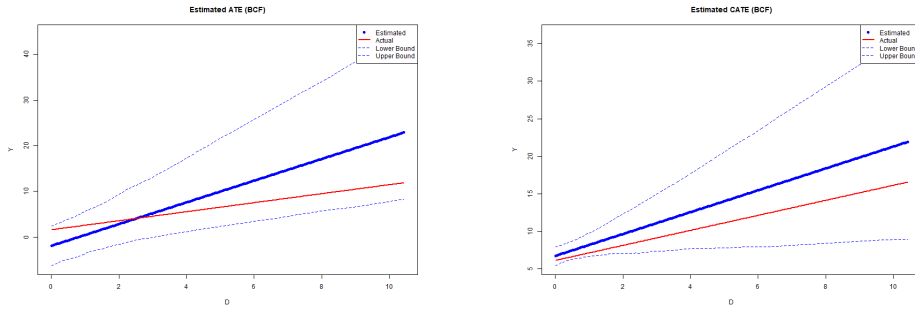


Figure 43: BCF ATE and CATE Functions Estimation for $N=100$ (for CATE, an Example of a Random \mathbf{x}_i of a Random Simulation is used)

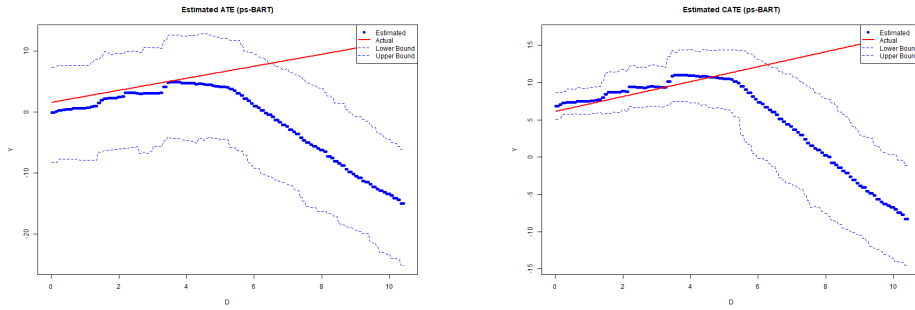


Figure 44: ps-BART ATE and CATE Functions Estimation for $N=100$ (for CATE, an Example of a Random \mathbf{x}_i of a Random Simulation is used)

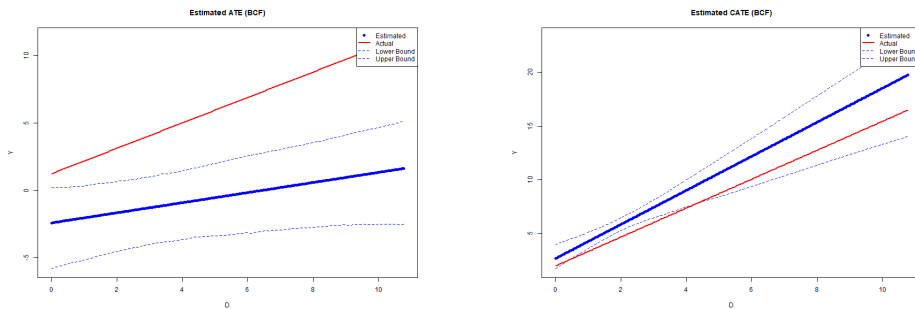


Figure 45: BCF ATE and CATE Functions Estimation for $N=250$ (for CATE, an Example of a Random \mathbf{x}_i of a Random Simulation is used)

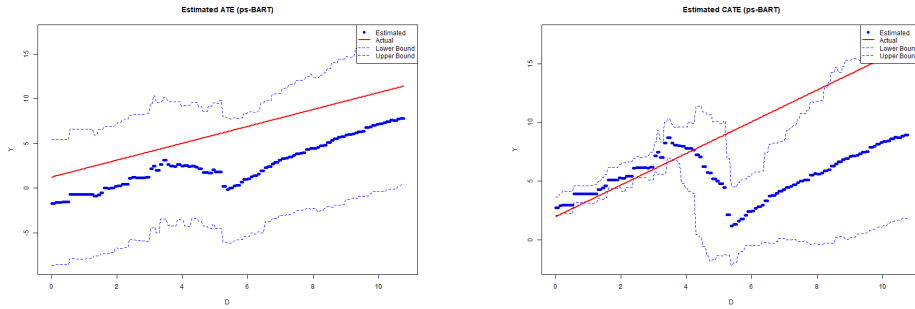


Figure 46: ps-BART ATE and CATE Functions Estimation for $N=250$ (for CATE, an Example of a Random x_i of a Random Simulation is used)

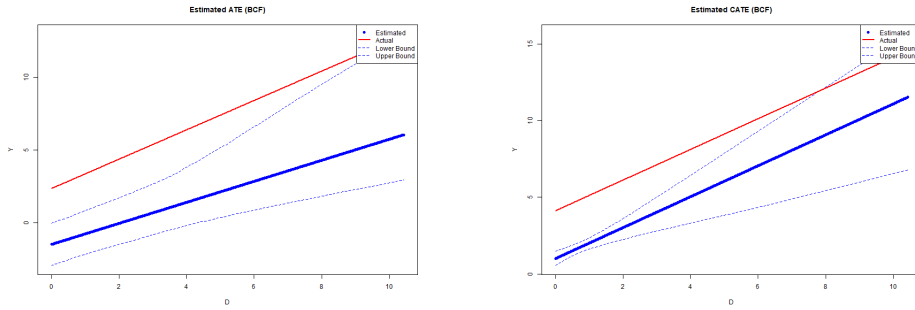


Figure 47: BCF ATE and CATE Functions Estimation for $N=500$ (for CATE, an Example of a Random x_i of a Random Simulation is used)

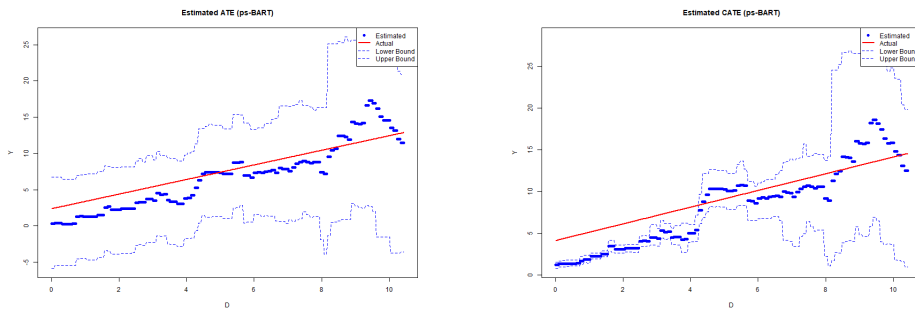


Figure 48: ps-BART ATE and CATE Functions Estimation for $N=500$ (for CATE, an Example of a Random x_i of a Random Simulation is used)

Table 30: Statistical Test Results: p-values for Different Metrics (n=100)

Metric	Fligner-Policello Test	Mann-Whitney U Test	Kruskal-Wallis H Test	Levene's Test	Brown-Forsythe Test
RMSE _{ATE} *	N/A	N/A	N/A	N/A	N/A
MAE _{ATE} *	N/A	N/A	N/A	N/A	N/A
MAPE _{ATE}	N/A	0.9231	0.9221	0.5095	0.6075
Len _{ATE}	1.40×10^{-72}	N/A	N/A	9.25×10^{-9}	1.54×10^{-6}
RMSE _{CATE}	4.98×10^{-28}	N/A	N/A	1.06×10^{-7}	3.46×10^{-5}
MAE _{CATE}	1.30×10^{-17}	N/A	N/A	3.51×10^{-7}	5.34×10^{-5}
MAPE _{CATE}	N/A	0.0959	0.0956	0.9890	0.9558
Len _{CATE}	N/A	0.3375	0.3369	0.7350	0.8401
SEC _{ATE}	1.86×10^{-20}	N/A	N/A	6.53×10^{-17}	3.54×10^{-5}
AEC _{ATE}	1.86×10^{-20}	N/A	N/A	2.72×10^{-21}	1.06×10^{-5}
SEC _{CATE}	N/A	0.1019	0.1016	0.5731	0.5961
AEC _{CATE} *	N/A	N/A	N/A	0.4287	N/A

*: RMSE_{ATE}, MAE_{ATE}, and AEC_{CATE} had p-values of 0.07, 0.77, and 0.06 for the T-test and 0.91, 0.39, and 0.43 for the F-test respectively.

Table 31: Statistical Test Results: p-values for Different Metrics (n=250)

Metric	Fligner-Policello Test	Mann-Whitney U Test	Kruskal-Wallis H Test	Levene's Test	Brown-Forsythe Test
RMSE _{ATE}	N/A	0.4165	0.4158	0.2550	0.2549
MAE _{ATE} *	N/A	N/A	N/A	N/A	N/A
MAPE _{ATE}	0.9001	N/A	N/A	0.0101	0.0110
Len _{ATE}	0	N/A	N/A	1.75×10^{-12}	6.51×10^{-12}
RMSE _{CATE}	1.83×10^{-185}	N/A	N/A	1.40×10^{-10}	3.77×10^{-7}
MAE _{CATE}	6.99×10^{-65}	N/A	N/A	3.00×10^{-11}	1.54×10^{-7}
MAPE _{CATE}	N/A	0.0035	0.0035	0.3926	0.4815
Len _{CATE}	5.15×10^{-47}	N/A	N/A	5.01×10^{-5}	5.82×10^{-4}
SEC _{ATE}	5.21×10^{-96}	N/A	N/A	5.26×10^{-57}	2.07×10^{-56}
AEC _{ATE}	5.21×10^{-96}	N/A	N/A	1.32×10^{-56}	3.23×10^{-41}
SEC _{CATE}	N/A	6.60×10^{-15}	6.53×10^{-15}	0.0703	0.1193
AEC _{CATE}	N/A	6.60×10^{-15}	6.53×10^{-15}	0.4335	0.6741

*: MAE_{ATE} had p-values of 0.86 for the T-test and 0.13 for the F-test.

Table 32: Statistical Test Results: p-values for Different Metrics (n=500)

Metric	Fligner-Policello Test	Mann-Whitney U Test	Kruskal-Wallis H Test	Levene's Test	Brown-Forsythe Test
RMSE _{ATE}	0.8134	N/A	N/A	0.0194	0.0493
MAE _{ATE}	0.9750	N/A	N/A	0.0364	0.0660
MAPE _{ATE}	N/A	0.9212	0.9202	0.3540	0.3766
Len _{ATE}	0	N/A	N/A	4.48×10^{-13}	9.27×10^{-11}
RMSE _{CATE}	0	N/A	N/A	1.89×10^{-18}	5.58×10^{-13}
MAE _{CATE}	0	N/A	N/A	7.70×10^{-19}	2.07×10^{-14}
MAPE _{CATE}	N/A	0.0023	0.0023	0.8456	0.8436
Len _{CATE}	0	N/A	N/A	2.65×10^{-14}	5.07×10^{-11}
SEC _{ATE}	0	N/A	N/A	3.03×10^{-29}	7.23×10^{-11}
AEC _{ATE}	0	N/A	N/A	2.34×10^{-17}	1.26×10^{-7}
SEC _{CATE} *	N/A	N/A	N/A	N/A	N/A
AEC _{CATE}	8.99×10^{-94}	N/A	N/A	0.0036	0.0114

*: SEC_{CATE} had p-values of 2.68×10^{-29} for the T-test and 0.24 for the F-test.

4.3.2 Nonlinear Relationship

Table 33 shows the performance measures results for the 3rd Set of DGPs with Nonlinear Relationship. For $n = 100$, it can be seen that both models have a similar performance and robustness for ATE function estimation regarding point-wise estimation, while the ps-BART model being slightly better and more robust for CATE function estimation. Table 34 shows that the similarity between the models is statistically significant for ATE function estimation while the slight superiority of the ps-BART model is not for CATE function estimation. Concerning uncertainty estimation, both models have a similar performance and robustness considering ATE function estimation (which is also confirmed by the results found in Table 34), while the benchmark model being statistically significantly better for CATE function estimation. For $n = 250$ and $n = 500$, both models still have a similar performance for ATE function estimation regarding point-wise estimation (which is confirmed by the results of Tables 35 and 36), but now the proposed model is statistically significantly more robust. Regarding point-wise CATE function estimation, the ps-BART model's advantage over the BCF model is now more pronounced, making it statistically significant. Regarding uncertainty estimation, the proposed model has a better performance and robustness considering ATE function estimation (though only statistically significant for $n = 250$), while the benchmark model being statistically significantly better for CATE function estimation.

Figures 49, 50, 51, 52, 53, and 54 graphically illustrate the results of Table 33. The misspecification of the BCF model for the underlying DGP can be visually seen in these figures.

Table 33: Metric Results

<i>n</i>	Metric	BCF (Mean \pm SD)	ps-BART (Mean \pm SD)
100	RMSE _{ATE}	2.914 \pm 0.859	2.861 \pm 0.802
	MAE _{ATE}	2.753 \pm 0.883	2.793 \pm 0.826
	MAPE _{ATE}	6.165 \pm 6.970	6.430 \pm 7.020
	Len _{ATE}	10.572 \pm 1.742	10.153 \pm 1.554
	Cover _{ATE}	0.953 \pm 0.155	0.958 \pm 0.162
	RMSE _{CATE}	4.600 \pm 0.779	4.337 \pm 0.467
	MAE _{CATE}	4.126 \pm 0.613	4.127 \pm 0.447
	MAPE _{CATE}	8.567 \pm 7.974	7.892 \pm 7.129
	Len _{CATE}	9.011 \pm 2.629	6.367 \pm 1.013
	Cover _{CATE}	0.561 \pm 0.092	0.451 \pm 0.071
	SEC _{ATE}	0.024 \pm 0.087	0.026 \pm 0.125
	AEC _{ATE}	0.086 \pm 0.128	0.078 \pm 0.143
	SEC _{CATE}	0.159 \pm 0.076	0.254 \pm 0.071
	AEC _{CATE}	0.389 \pm 0.092	0.499 \pm 0.071
250	RMSE _{ATE}	3.044 \pm 0.778	2.986 \pm 0.590
	MAE _{ATE}	2.859 \pm 0.806	2.936 \pm 0.596
	MAPE _{ATE}	7.492 \pm 16.323	7.932 \pm 12.287
	Len _{ATE}	9.743 \pm 1.498	10.254 \pm 1.733
	Cover _{ATE}	0.902 \pm 0.198	0.972 \pm 0.109
	RMSE _{CATE}	4.909 \pm 0.985	4.135 \pm 0.328
	MAE _{CATE}	4.326 \pm 0.782	3.959 \pm 0.310
	MAPE _{CATE}	8.324 \pm 3.958	7.346 \pm 3.948
	Len _{CATE}	7.376 \pm 1.853	4.924 \pm 0.767
	Cover _{CATE}	0.462 \pm 0.063	0.363 \pm 0.056
	SEC _{ATE}	0.041 \pm 0.098	0.012 \pm 0.076
	AEC _{ATE}	0.123 \pm 0.162	0.060 \pm 0.094
	SEC _{CATE}	0.242 \pm 0.062	0.347 \pm 0.064
	AEC _{CATE}	0.488 \pm 0.063	0.587 \pm 0.056
500	RMSE _{ATE}	3.132 \pm 0.935	3.037 \pm 0.664
	MAE _{ATE}	2.884 \pm 0.995	2.995 \pm 0.667
	MAPE _{ATE}	8.715 \pm 9.356	11.079 \pm 14.312
	Len _{ATE}	9.220 \pm 1.675	10.365 \pm 1.716
	Cover _{ATE}	0.859 \pm 0.260	0.982 \pm 0.060
	RMSE _{CATE}	5.284 \pm 1.186	4.060 \pm 0.454
	MAE _{CATE}	4.586 \pm 0.933	3.904 \pm 0.380
	MAPE _{CATE}	9.458 \pm 7.254	8.290 \pm 5.972
	Len _{CATE}	6.122 \pm 1.485	4.185 \pm 0.853
	Cover _{CATE}	0.375 \pm 0.049	0.303 \pm 0.063
	SEC _{ATE}	0.075 \pm 0.172	0.005 \pm 0.018
	AEC _{ATE}	0.154 \pm 0.228	0.053 \pm 0.042
	SEC _{CATE}	0.333 \pm 0.057	0.423 \pm 0.080
	AEC _{CATE}	0.575 \pm 0.049	0.647 \pm 0.063

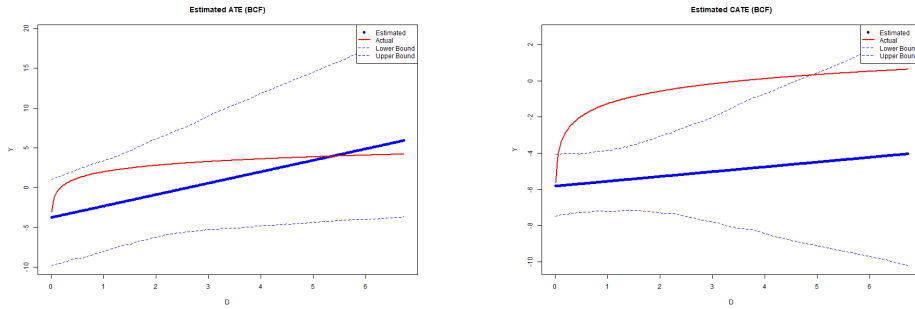


Figure 49: BCF ATE and CATE Functions Estimation for $N=100$ (for CATE, an Example of a Random \mathbf{x}_i of a Random Simulation is used)

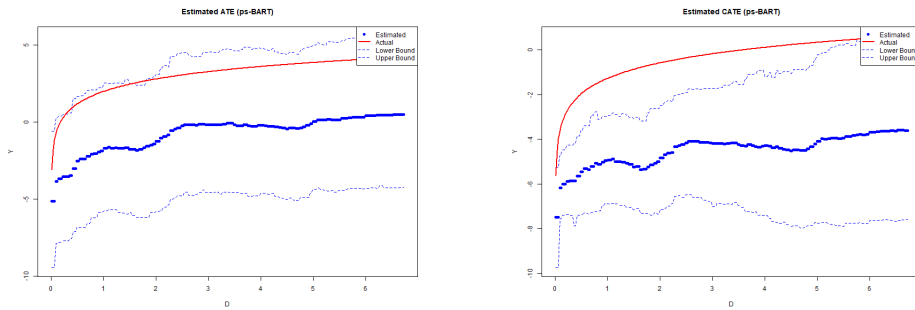


Figure 50: ps-BART ATE and CATE Functions Estimation for $N=100$ (for CATE, an Example of a Random \mathbf{x}_i of a Random Simulation is used)

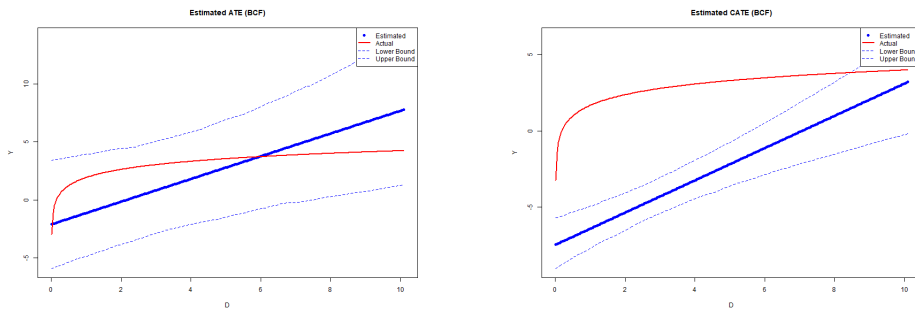


Figure 51: BCF ATE and CATE Functions Estimation for $N=250$ (for CATE, an Example of a Random \mathbf{x}_i of a Random Simulation is used)

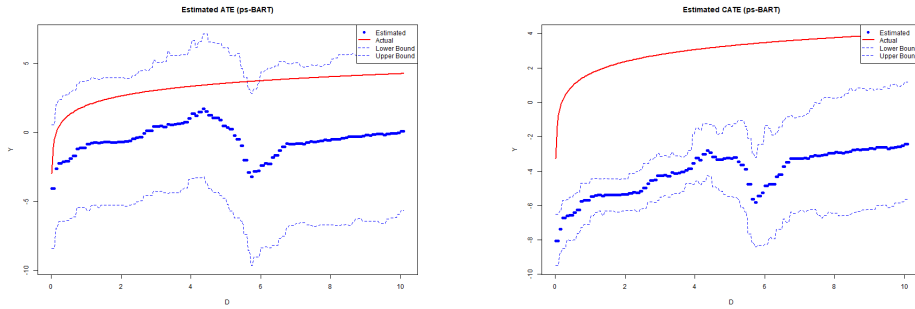


Figure 52: ps-BART ATE and CATE Functions Estimation for $N=250$ (for CATE, an Example of a Random \mathbf{x}_i of a Random Simulation is used)

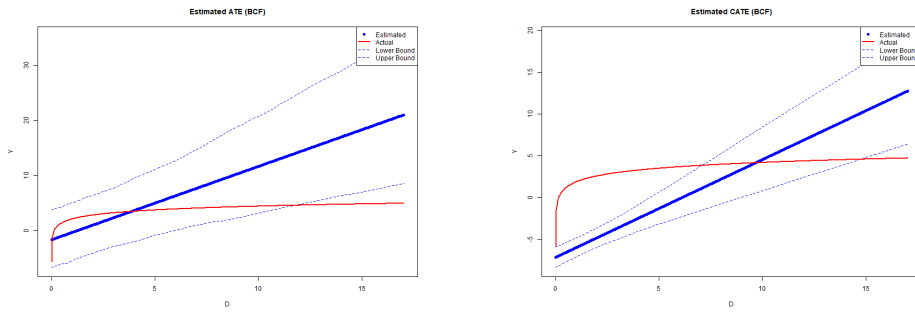


Figure 53: BCF ATE and CATE Functions Estimation for $N=500$ (for CATE, an Example of a Random \mathbf{x}_i of a Random Simulation is used)

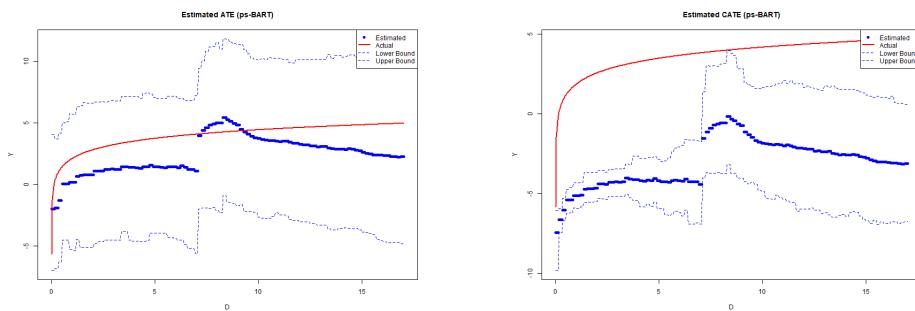


Figure 54: ps-BART ATE and CATE Functions Estimation for $N=500$ (for CATE, an Example of a Random \mathbf{x}_i of a Random Simulation is used)

Table 34: Statistical Test Results: p-values for Different Metrics (n=100)

Metric	Fligner-Policello Test	Mann-Whitney U Test	Kruskal-Wallis H Test	Levene's Test	Brown-Forsythe Test
RMSE _{ATE}	N/A	0.9659	0.9649	0.8676	0.9111
MAE _{ATE}	N/A	0.3958	0.3952	0.8342	0.8786
MAPE _{ATE}	N/A	0.2721	0.2715	0.8261	0.8958
Len _{ATE}	N/A	0.0954	0.0952	0.3249	0.3676
RMSE _{CATE}	0.0203	N/A	N/A	0.0010	0.0112
MAE _{CATE}	0.3959	N/A	N/A	0.0458	0.1266
MAPE _{CATE}	N/A	0.1518	0.1515	0.7203	0.7876
Len _{CATE}	1.61×10^{-36}	N/A	N/A	1.08×10^{-9}	9.84×10^{-9}
SEC _{ATE}	N/A	0.1260	0.1256	0.6469	0.8582
AEC _{ATE}	N/A	0.1260	0.1256	0.5490	0.8137
SEC _{CATE}	N/A	6.08×10^{-16}	6.02×10^{-16}	0.8055	0.9724
AEC _{CATE}	8.29×10^{-29}	N/A	N/A	0.0364	0.0445

Table 35: Statistical Test Results: p-values for Different Metrics (n=250)

Metric	Fligner-Policello Test	Mann-Whitney U Test	Kruskal-Wallis H Test	Levene's Test	Brown-Forsythe Test
RMSE _{ATE}	0.7607	N/A	N/A	0.0256	0.0342
MAE _{ATE}	0.3566	N/A	N/A	0.0128	0.0165
MAPE _{ATE}	N/A	0.0182	0.0181	0.6651	0.7818
Len _{ATE}	N/A	0.0330	0.0329	0.1170	0.1303
RMSE _{CATE}	3.43×10^{-24}	N/A	N/A	6.36×10^{-10}	1.80×10^{-7}
MAE _{CATE}	6.63×10^{-4}	N/A	N/A	9.24×10^{-8}	6.09×10^{-6}
MAPE _{CATE}	N/A	0.0094	0.0093	0.3417	0.4743
Len _{CATE}	1.42×10^{-79}	N/A	N/A	6.56×10^{-11}	4.04×10^{-10}
SEC _{ATE}	4.49×10^{-5}	N/A	N/A	9.20×10^{-5}	0.0237
AEC _{ATE}	4.49×10^{-5}	N/A	N/A	9.14×10^{-9}	0.0034
SEC _{CATE} *	N/A	N/A	N/A	N/A	N/A
AEC _{CATE} *	N/A	N/A	N/A	N/A	N/A

*: SEC_{CATE} and AEC_{CATE} had p-values of 1.67×10^{-24} and 3.07×10^{-24} for the T-test and 0.65 and 0.25 for the F-test respectively.

Table 36: Statistical Test Results: p-values for Different Metrics (n=500)

Metric	Fliqner-Policello Test	Mann-Whitney U Test	Kruskal-Wallis H Test	Levene's Test	Brown-Forsythe Test
RMSE _{ATE}	0.8850	N/A	N/A	0.0128	0.0149
MAE _{ATE}	0.0456	N/A	N/A	0.0008	0.0011
MAPE _{ATE}	N/A	0.0370	0.0369	0.2122	0.4973
Len _{ATE}	N/A	1.88×10^{-6}	1.87×10^{-6}	0.8948	0.8562
RMSE _{CATE}	3.60×10^{-84}	N/A	N/A	6.35×10^{-10}	8.42×10^{-8}
MAE _{CATE}	9.01×10^{-17}	N/A	N/A	1.42×10^{-8}	1.07×10^{-6}
MAPE _{CATE}	N/A	0.0014	0.0014	0.5627	0.6286
Len _{CATE}	1.99×10^{-66}	N/A	N/A	4.16×10^{-5}	1.28×10^{-4}
SEC _{ATE}	0.6648	N/A	N/A	2.10×10^{-15}	5.91×10^{-5}
AEC _{ATE}	0.6648	N/A	N/A	5.06×10^{-19}	7.21×10^{-6}
SEC _{CATE}	9.40×10^{-27}	N/A	N/A	0.0026	0.0055
AEC _{CATE} *	N/A	N/A	N/A	N/A	N/A

*: AEC_{CATE} had p-values of 2.18×10^{-16} for the T-test and 0.02 for the F-test.

4.3.3 Conclusion

The results of this set of DGPs demonstrate the fact that (semi-)parametric models outperform nonparametric models when correctly specified for the underlying DGP (Jabot, 2015; W. Liu & Yang, 2011; Robinson, 2010). However, the BCF model is interestingly superior to the ps-BART model in uncertainty estimation for the CATE function estimation for the Nonlinear Relationship DGP while being worse in point-wise estimation. However, this can be easily explained by the fact that the BCF model is using considerably larger confidence interval lengths than the ps-BART model, creating the false impression that the BCF model has a better uncertainty estimation for the CATE function estimation. Lastly, the results of this set of DGPs confirm the hypothesis that for significantly nonlinear DGPs the ps-BART model becomes more robust than the BCF model due to the considerably misspecification of the latter while for slightly nonlinear/considerably linear DGPs, the benchmark model is more robust.

5 Conclusion

This paper presents a significant advancement in the literature on causal inference, particularly in the estimation of ATE and CATE for continuous treatments. The proposed generalized ps-BART model effectively addresses the limitations of the BCF model by offering a more flexible and accurate approach to capturing the potentially nonlinear and complex relationships between the treatment, covariates, and outcome variables. The nonparametric nature of the ps-BART model provides several advantages over its benchmark counterpart, including its ability to adapt to a variety of functional forms, its reduced risk of misspecification, and its suitability across a wide range of DGPs, increasing its potential use in the Health and Social Sciences research.

The experimental results of this paper, based on three distinct sets of DGPs, further highlight the strengths of the ps-BART model relative to the BCF model. It is worth remembering that when we say below that a DGP is (non)linear, we mean that the DGP has a (non)linear relationship between the treatment and outcome.

For moderately nonlinear DGPs (i.e., the first set of DGPs), the ps-BART model consistently outperforms the BCF model in both point-wise and uncertainty estimation of ATE and CATE functions, though only for when the sample size is $n \geq 250$ for slightly nonlinear DGPs (i.e., when the semi-parametric assumption of the BCF model is not far off from the true DGP). Interestingly, while the BCF model demonstrated more robustness in ATE point-wise estimation in slightly nonlinear scenarios, this performance edge is attributable to the benchmark model's slightly alignment with linearity assumptions in these DGPs (where the relationship between the treatment and outcome becomes linear for high treatment doses). Nonetheless, the proposed model's flexibility gives it a distinct advantage in capturing even subtle nonlinear effects, which positions ps-BART as the more reliable model for most real-world data where the true functional form is not strictly linear.

In highly nonlinear DGPs (i.e., the second set of DGPs), the ps-BART model demonstrated clear superiority in both point-wise and uncertainty estimation. The flexibility of the ps-BART model allowed it to handle the complex relationships between

the treatment and outcome more effectively than the BCF model, which exhibited significant performance degradation due to misspecification. Interestingly, in this set of DGPs, the ps-BART model also proved to be more robust than the BCF model in both ATE and CATE estimation, further demonstrating that for significantly nonlinear DGPs the ps-BART model becomes more robust than the BCF model due to the considerably misspecification of the latter while for slightly nonlinear/considerably linear DGPs, the benchmark model is more robust

Regarding the third set of DGPs considered in this study, it can be seen that in cases where the DGP aligns closely with the parametric assumptions underlying the BCF model, as expected, the BCF model performed better in point-wise estimation of the ATE and CATE functions, as already expected from the theory (Jabot, 2015; W. Liu & Yang, 2011; Robinson, 2010). However, the results also showed that the BCF model achieved better uncertainty estimation in CATE for certain the nonlinear DGP considered in the third set of DGPs, which was largely due to its reliance on overly wide confidence intervals. This gave the false impression of more accurate uncertainty estimation, when in reality, the ps-BART model provided tighter intervals that more accurately reflected the underlying distribution of the treatment effect. These results reaffirm the hypothesis that ps-BART is better suited for nonlinear DGPs, whereas the BCF model maintains some advantages in linear DGPs.

Hence, this research addresses a critical gap in the current literature on causal inference for continuous treatments by providing a fully nonparametric model that avoids the restrictive assumptions imposed by parametric or semi-parametric models such as the BCF model. The ps-BART model's ability to provide accurate and flexible estimates of ATE and CATE functions, while simultaneously offering probabilistic estimation through uncertainty quantification, makes it a valuable addition to the toolkit for causal inference. The development of this model represents a key step toward closing the gap in probabilistic estimation of causal effects for continuous treatments, where existing the existing benchmark model fails to provide reliable estimates for when the relationship between the treatment and outcome is nonlinear. By introducing a more flexible alternative, this research opens up new avenues for further exploration in the field and the application of the proposed model in the Health and Social Sciences literature.

Finally, regarding causal inference research (i.e., the research to create the tools to properly perform causal inference), several future research directions emerge from the results of this study. Firstly, the ps-BART model could be extended to handle time-varying treatments, where the treatment and outcome are observed over multiple time points. The flexibility of the model positions it well for this task, which could further expand its applicability in real-world scenarios such as clinical trials or longitudinal studies. Additionally, future research could explore the performance of the ps-BART model in high-dimensional covariate spaces, where feature selection and model regularization play crucial roles. Understanding how the proposed model performs under different regularization strategies in high-dimensional settings would be valuable for extending its use to large-scale observational studies. Finally, future research could investigate optimal hyperparameter and prior tuning for ps-BART using cross-validation techniques to further enhance the model's performance across different DGPs.

6 Supplementary Research Material and Code

The supplementary research material and code used in this paper can be found in the following GitHub repository:

References

- Bembom, O., & van der Laan, M. J. (2007). A practical illustration of the importance of realistic individualized treatment rules in causal inference. *Electronic Journal of Statistics*, 1(none). <https://doi.org/10.1214/07-ejs105>
- Cai, Z., & Hong, Y. (2003). Nonparametric methods in continuous-time finance: A selective review. In *Recent advances and trends in nonparametric statistics* (pp. 283–302). Elsevier. <https://doi.org/10.1016/b978-044451378-6/50019-3>
- Chernozhukov, V., Hansen, C., Kallus, N., Spindler, M., & Syrgkanis, V. (2024). *Applied causal inference powered by ml and ai*. Online.
- Chipman, H. A., George, E. I., & McCulloch, R. E. (2010). Bart: Bayesian additive regression trees. *The Annals of Applied Statistics*, 4(1). <https://doi.org/10.1214/09-aos285>
- Crown, W. H. (2019). Real-world evidence, causal inference, and machine learning. *Value in Health*, 22(5), 587–592. <https://doi.org/10.1016/j.jval.2019.03.001>
- Cui, P., Shen, Z., Li, S., Yao, L., Li, Y., Chu, Z., & Gao, J. (2020). Causal inference meets machine learning, 3527–3528. <https://doi.org/10.1145/3394486.3406460>
- Curth, A., & van der Schaar, M. (2021, 13–15 Apr). Nonparametric estimation of heterogeneous treatment effects: From theory to learning algorithms. In A. Banerjee & K. Fukumizu (Eds.), *Proceedings of the 24th international conference on artificial intelligence and statistics* (pp. 1810–1818, Vol. 130). PMLR. <https://proceedings.mlr.press/v130/curth21a.html>
- Grimmer, J. (2014). We are all social scientists now: How big data, machine learning, and causal inference work together. *PS: Political Science & Politics*, 48(01), 80–83. <https://doi.org/10.1017/s1049096514001784>
- Hahn, P. R., Carvalho, C. M., Puelz, D., & He, J. (2018). Regularization and confounding in linear regression for treatment effect estimation. *Bayesian Analysis*, 13(1). <https://doi.org/10.1214/16-ba1044>
- Hahn, P. R., Murray, J. S., & Carvalho, C. M. (2020). Bayesian regression tree models for causal inference: Regularization, confounding, and heterogeneous effects (with discussion). *Bayesian Analysis*, 15(3). <https://doi.org/10.1214/19-ba1195>
- Hayashi, K., Bentler, P. M., & Yuan, K.-H. (2011). Structural equation modeling. In *Essential statistical methods for medical statistics* (pp. 202–234). Elsevier. <https://doi.org/10.1016/b978-0-444-53737-9.50010-4>
- Hirano, K., & Imbens, G. W. (2004, July). The propensity score with continuous treatments. <https://doi.org/10.1002/0470090456.ch7>

- Jabot, F. (2015). Why preferring parametric forecasting to nonparametric methods? *Journal of Theoretical Biology*, 372, 205–210. <https://doi.org/10.1016/j.jtbi.2014.07.038>
- Kennedy, E. H. (2020). Towards optimal doubly robust estimation of heterogeneous causal effects. <https://doi.org/10.48550/ARXIV.2004.14497>
- Kennedy, E. H., Ma, Z., McHugh, M. D., & Small, D. S. (2016). Non-parametric methods for doubly robust estimation of continuous treatment effects. *Journal of the Royal Statistical Society Series B: Statistical Methodology*, 79(4), 1229–1245. <https://doi.org/10.1111/rssb.12212>
- Kuang, K., Li, L., Geng, Z., Xu, L., Zhang, K., Liao, B., Huang, H., Ding, P., Miao, W., & Jiang, Z. (2020). Causal inference. *Engineering*, 6(3), 253–263. <https://doi.org/10.1016/j.eng.2019.08.016>
- Künzel, S. R., Sekhon, J. S., Bickel, P. J., & Yu, B. (2019). Metalearners for estimating heterogeneous treatment effects using machine learning. *Proceedings of the National Academy of Sciences*, 116(10), 4156–4165. <https://doi.org/10.1073/pnas.1804597116>
- Lee, Y.-Y. (2018). Partial mean processes with generated regressors: Continuous treatment effects and nonseparable models. <https://doi.org/10.48550/ARXIV.1811.00157>
- Liu, W., & Yang, Y. (2011). Parametric or nonparametric? a parametricness index for model selection. *The Annals of Statistics*, 39(4). <https://doi.org/10.1214/11-aos899>
- Liu, X. (2016). Special topics on linear mixed models. In *Methods and applications of longitudinal data analysis* (pp. 205–242). Elsevier. <https://doi.org/10.1016/b978-0-12-801342-7.00007-1>
- Martin, R., & Syring, N. (2022). Direct gibbs posterior inference on risk minimizers: Construction, concentration, and calibration. In *Advancements in bayesian methods and implementation* (pp. 1–41). Elsevier. <https://doi.org/10.1016/bs.host.2022.06.004>
- Moodie, E. E., & Stephens, D. A. (2010). Estimation of dose–response functions for longitudinal data using the generalised propensity score. *Statistical Methods in Medical Research*, 21(2), 149–166. <https://doi.org/10.1177/0962280209340213>
- Murnane, R. J., & Willett, J. B. (2010). *Methods matter: Improving causal inference in educational and social science research*. Oxford University Press.
- Nie, X., & Wager, S. (2017). Quasi-oracle estimation of heterogeneous treatment effects. <https://doi.org/10.48550/ARXIV.1712.04912>
- Ohlsson, H., & Kendler, K. S. (2020). Applying causal inference methods in psychiatric epidemiology: A review. *JAMA Psychiatry*, 77(6), 637. <https://doi.org/10.1001/jamapsychiatry.2019.3758>
- Robinson, P. (2010). Efficient estimation of the semiparametric spatial autoregressive model. *Journal of Econometrics*, 157(1), 6–17. <https://doi.org/10.1016/j.jeconom.2009.10.031>
- Rothenhäusler, D., & Yu, B. (2019). Incremental causal effects. <https://doi.org/10.48550/ARXIV.1907.13258>

- Sobel, M. E. (2000). Causal inference in the social sciences. *Journal of the American Statistical Association*, 95(450), 647–651. <https://doi.org/10.1080/01621459.2000.10474243>
- Souto, H. G., & Neto, F. L. (2024). Really doing great at model evaluation for cate estimation? a critical consideration of current model evaluation practices in treatment effect estimation. <https://doi.org/10.48550/ARXIV.2409.05161>
- Woody, S., Carvalho, C. M., Hahn, P. R., & Murray, J. S. (2020). Estimating heterogeneous effects of continuous exposures using bayesian tree ensembles: Revisiting the impact of abortion rates on crime. <https://doi.org/10.48550/ARXIV.2007.09845>
- Wu, X., Mealli, F., Kioumourtzoglou, M.-A., Dominici, F., & Braun, D. (2022). Matching on generalized propensity scores with continuous exposures. *Journal of the American Statistical Association*, 119(545), 757–772. <https://doi.org/10.1080/01621459.2022.2144737>
- Yao, L., Chu, Z., Li, S., Li, Y., Gao, J., & Zhang, A. (2021). A survey on causal inference. *ACM Transactions on Knowledge Discovery from Data*, 15(5), 1–46. <https://doi.org/10.1145/3444944>